UNIVERSITY OF CRETE

SCHOOL OF SCIENCE AND ENGINEERING

DEPARTMENT OF CHEMISTRY

Department of Materials Science and Technology, Laboratory of Synthetic Biomaterials

Supervisor Dr. Kelly Velonia

Department of Chemistry, Laboratory of Bioinorganic Chemistry

Supervisor: Dr. Athanasios G. Koutsolelos

Bachelor Thesis

"Synthesis of Multifunctional Protein-Porphyrin Bioconjugates"

By

Petros Mandriotis

(AM: 1989)

Abstract
Porphyrins are highly important compounds found in plants and animals. These tetrapyrolic molecules are of central importance in metabolic processes, including electron transfer during respiration, photosynthesis, and enzyme catalysis. The most notable representatives are chlorophyll in the plant kingdom and haemoglobin in the animal kingdom.
The following work focuses on certain porphyrin conjugated proteins named hemeproteins as well as the synthesis of a hybrid hemeprotein through BSA-Tetraphenylporphyrin maleimide coupling. The main purpose of the thesis was the synthesis of a hybrid hemeprotein and the investigation of its catalytic properties and more specifically if it possessed stereoselectivity. Moreover, a secondary purpose was to investigate whether the hybrid hemeprotein exhibited oxygen carrying properties. Despite all our effort we were able to synthesize only the hybrid hemeprotein

Σύνοψη

Οι πορφυρίνες αποτελούν σημαντικές ενώσεις σε ζώα και φυτά. Οι τετραπυρολικές αυτές ενώσεις συντελούν σε μεταβολικές διεργασίες όπως μεταφορά ηλεκτρονίων κατά την κυτταρική αναπνοή, φωτοσύνθεση, και ενζυμική κατάλυση. Ίσως οι πιο γνωστές ενώσεις πορφυρίνης στη φύση είναι η χλωροφύλλη όσον αφορά το φυτικό βασίλειο και η αιμοσφαιρίνη όσον αφορά το ζωικό βασίλειο.
Η εργασία που ακολουθεί αποσκοπεί επικεντρώνεται σε ενώσεις πορφυρίνης-πρωτεΐνης που ονομάζονται αιμοπρωτεΐνες και πιο συγκεκριμένα στη σύνθεση μιας υβριδικής αιμοπρωτεΐνης μέσω μέσω σύζευξης της BSA και της τετραφαίνυλοπορφυρίνης χρησιμοποιώντας χημεία μαλειμιδίου. Ο κύριος σκοπός της διπλωματικής εργασίας ήταν η σύνθεση της υβριδικής αιμοπρωτεΐνης και η μελέτη των καταλυτικών ιδιοτήτων της. Δευτερεύων σκοπός ήταν η μελέτη ως προς την μεταφορά οξυγόνου. Παρά τις προσπάθειες μας επιτεύχθηκε μόνο η σύνθεση της υβριδικης αιμοπρωτεΐνης.

Contents

Acknowledgements

I would like to thank my supervisors, Dr. Kelly Velonia and Dr. Athanasios G Coutsolelos, for the patient guidance, encouragement and advice they provided throughout my time in the laboratory. I have been extremely lucky to have supervisors who cared so much about my work, and who responded to my questions and queries so promptly. I would also like to thank Dr. Georgios Charalambidis, Dr. Alexis Theodorou and MSc student Adelaida Trapali who helped me in my supervisor's absence.

Completing this work would have been all the more difficult were it not for the support and friendship provided by the other members of the laboratory. In particular I would like to thank Eva Grafanaki, Maria Papageorgiou, Sokratis Kalfaoglou, Panagiotis Skordalidis and Nikos Andrikopoulos for the pleasant workplace atmosphere, stimulating discussions and all the fun in the last 6 months.

Abbreviations

BSA	Bovine Serum Albumin
DMSO	Dimethyl Sulfoxide
GPC	Gel Permeation Chromatography
UV Vis	Ultra Violet Visible
TLC	Thin Layer Chromatography
PAGE	Polyacrylamide Gel Electrophoresis
H_2O_2	Hydrogen peroxide
O_2	Molecular oxygen
IR	Infrared
MALDI-TOF	Matrix Assisted Laser Desorption Ionization - Time of Flight
DCM	Dichloromethane
TCEP	Tris(2-Carboxyethyl)phosphine
MEOH	Methanol
$Na_2S_2O_4$	Sodium dithionite

1.0 Introduction

Hemeproteins are one of the most important families of compounds known in biochemistry. They are widely found in aerobic organisms and their functions include oxygen transport and storage, electron transfer in cellular oxidation processes and the catalytic decomposition of H_2O_2. Hemeproteins consist of a porphyrin-iron prosthetic group, called heme (Figure 1), which is conjugated to a protein.[1] Due to the multiple functions of the heme molecule, hemeproteins are being targeted for protein design.[2]

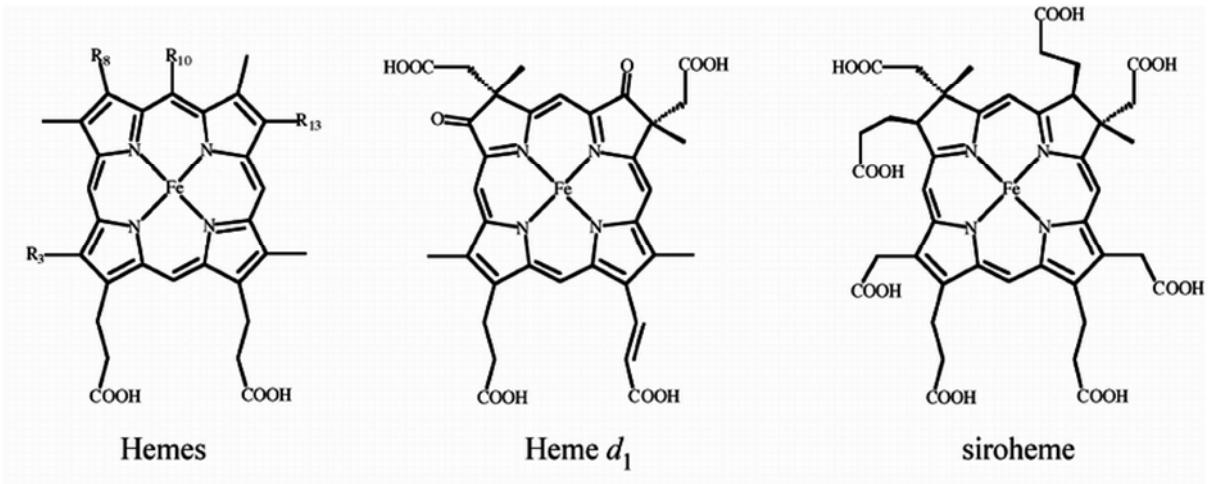

Heme type	Porphyrin ring substituents			
	R_3	R_8	R_{10}	R_{13}
heme *a*	formyl	hydroxyethylfarnesyl	hydrogen	vinyl
heme *b*	methyl	vinyl	hydrogen	vinyl
heme *c*	methyl	thioether	hydrogen	thioether
heme *o*	methyl	hydroxyethylfarnesyl	hydrogen	vinyl
P460	methyl	thioether	tyrosine	thioether
Fe(coproporphyrin)	methyl	propionic acid	hydrogen	propionic acid

Figure 1 Major heme groups found in nature[41]

1.1 Globin family

Hemoglobins are a sub-family of hemeproteins that reversibly bind O_2 through the heme group. Such hemeproteins have been identified in bacteria, plants, fungi and animals where their function is to supply O_2 as part of the respiratory chain.[3]

Structural bases of globin action

The tertiary globin structure is based on a seven/eight-helix arrangement otherwise known as globin fold where the heme group is found in a deep incision within the protein scaffold. Non covalent bonds between Fe and Histidine provide additional stability to the heme group. Oxygen is only able to bind to Fe on one side of the heme plane which is closest to the E helicase due to the fact that F8 Histidine blocks the binding from the opposite side (Figure 2). Reversible oxygen binding is caused by heme oxidation where the heme-Fe atom switches conformation from pentacoordinated to hexacoordinated.[3]

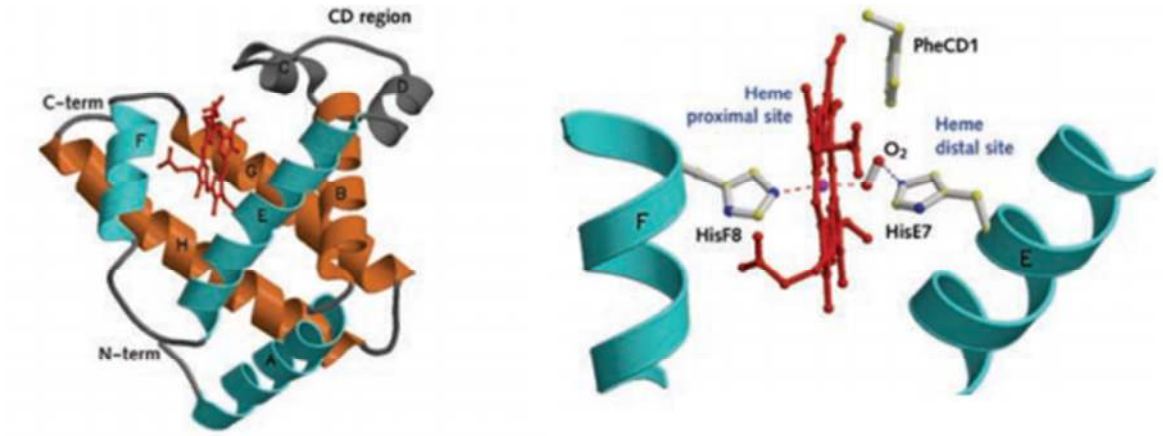

Figure 2 Globin structure. [3]

Studies have shown that the bond angle of Fe-Ô-O is 136° and the bond length Fe-O is 1,75Å, a value 0,1 Å smaller than the sum of the atomic radii which means a presence of double bond character which arises from d-p back bonding (Figure 3).[4]

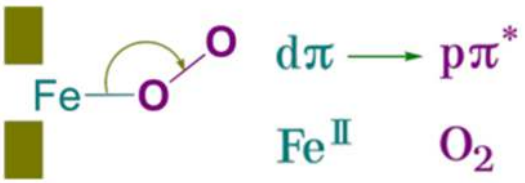

Figure 3 Iron oxygen bonding. [4]

1.1.1 Hemoglobin and myoglobin

Human myoglobin, a monomeric hemeprotein composed of 153 amino acids is mainly found in muscle tissue where it functions as a intracellular storage unit for oxygen. Adult human hemoglobin is a tetrameric hemeprotein with 2 alpha chains, each containing 144 amino acids and 2 beta chains, each containing consisting 146 amino acids.[5] It is found in erythrocytes where it functions by binding to oxygen in the lung and transporting it throughout the body where it will be used in areobic pathways.[6]

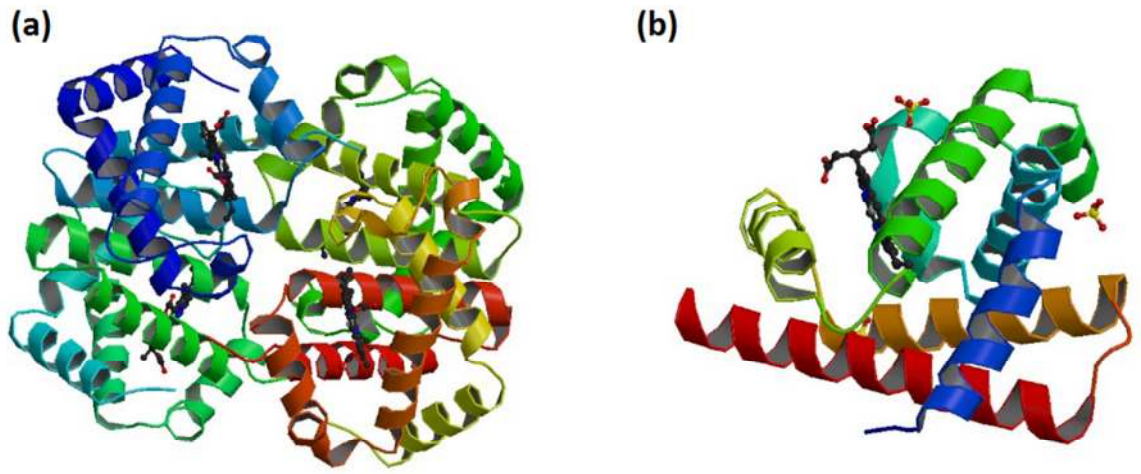

Figure 4 (a) Deoxy human hemoglobin and (b) human myoglobin.[7]

Although the secondary and tertiary structure of myoglobin and hemoglobin appear similar (Figure 5), the variation in the amino acid sequences marks the difference in hemeoglobin's oxygen carrying properties. In addition unlike myoglobin, hemoglobin possesses a quaternary structure that leads to important allosteric interactions between subunits.[6]

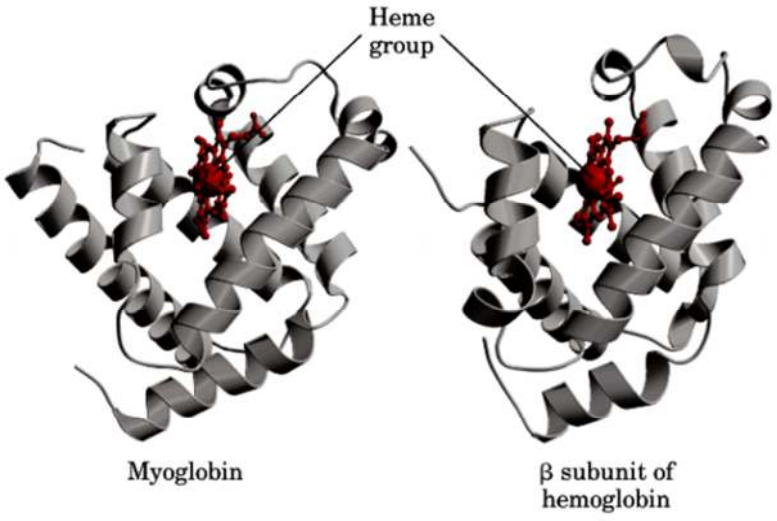

Figure 5 Visual comparison of myoblobin structure to the beta subunit of haemoglobin.[4]

1.1.2 Cytoglobin and neuroglobin

Cytoglobin and neuroglobin are both monomeric intracellular hemeproteins. Human neuroglobin, consisting of roughly 150 amino acids is mainly expressed in nerve cells and it is thought to protect neurons from hypoxic–ischemic injury. Cytoglobin on the other hand is expressed in many different tissues and consists of 190 amino acid residues (Figure 6). The roles of both neuroglobin and cytoglobin are not yet completely understood. Although oxygen supply is the most likely function, it is also possible that both globins act as O_2-consuming enzymes or as O_2 sensors.[3]

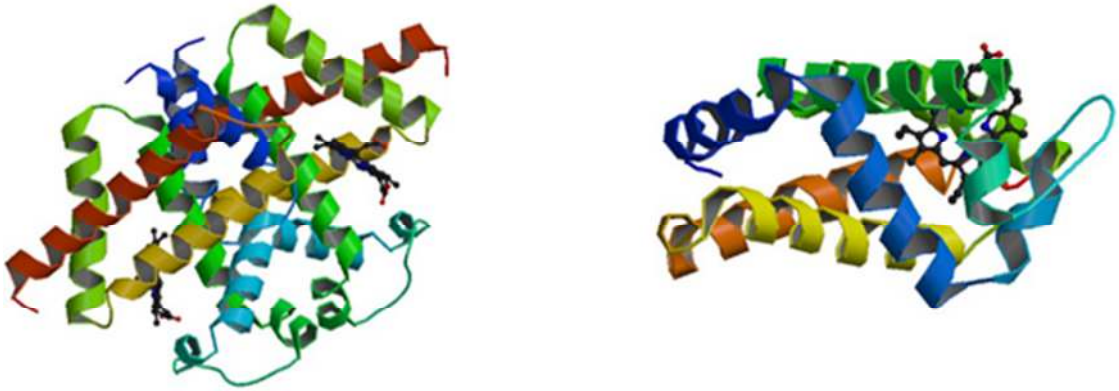

Figure 6 (Left) Human cytoglobin (ferric form) and (Right) human brain neuroglobin.[7]

The current chapter emphasized on mammalian globins and to be more precise, human globins. Globins can also be found in legume, a plant in the family of Fabaceae (commonly known as bean family). Well known legumes bearing globins include alfalfa, clover, peas, beans, chickpeas, lentils, lupin bean, mesquite, carob, soybeans, peanuts and tamarind. The following globin molecule, leghemoglobin is found in such plants. [8]

1.1.3 Leghemoglobin

Leghemoglobin is a hemeprotein found in infected cells of legume root and functions as part of nitrogen fixation process in legumes. The symbiotic existence of bacteria and plants results in the production of this specific protein, which not only protects the nitrogenase enzyme of denaturation under atmospheric oxygen concentration, but also supplies a sufficient amount of oxygen to the bacteria for respiration. Leghemoglobin is a monomeric protein and the amino acid sequence depends on the legume species despite the fact that the heme prosthetic group is preserved[9]

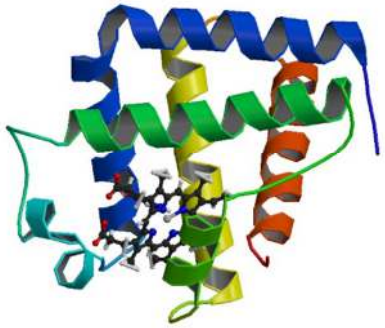

Figure 7 Ferric soybean leghemoglobin complexed with nicotinate.[7]

1.2 Electron transfer hemeproteins

Hemeproteins that facilitate electron transfer belong to the cytochrome family. Cytochromes are intracellular hemeproteins that undergo redox reactions and upon reduction exhibit intense absorption between 510-615 nm. They are subdivided into four classes depending on their light absorption spectra (figure 8).

Cytochrome	α band of pyridine ferrohemochrome in alkaline solution
Group *a*	580-590 nm
Group *b*	556-558 nm
Group *c*	549-551 nm (two thioether links) 553 nm (single thioether link)
Group *d*	600-620 nm

Figure 8 Major cytochrome groups.[10]

The four major groups of cytochromes (Figure 9) are**:**

Cytochromes *a*. Cytochromes in which the prosthetic group is heme *a*

Cytochromes *b*. Cytochromes in which the prosthetic group is heme b that is not covalently bound to the protein moiety

Cytochromes *c*. Cytochromes with thioether bonds between either or both of the vinyl side chains of the protoheme side chains and the protein.

Cytochromes *d*. Cytochromes with a tetrapyrolic chelate of iron as prosthetic group in which the degree of conjugation of double bonds is less than that in the porphyrin.[10]

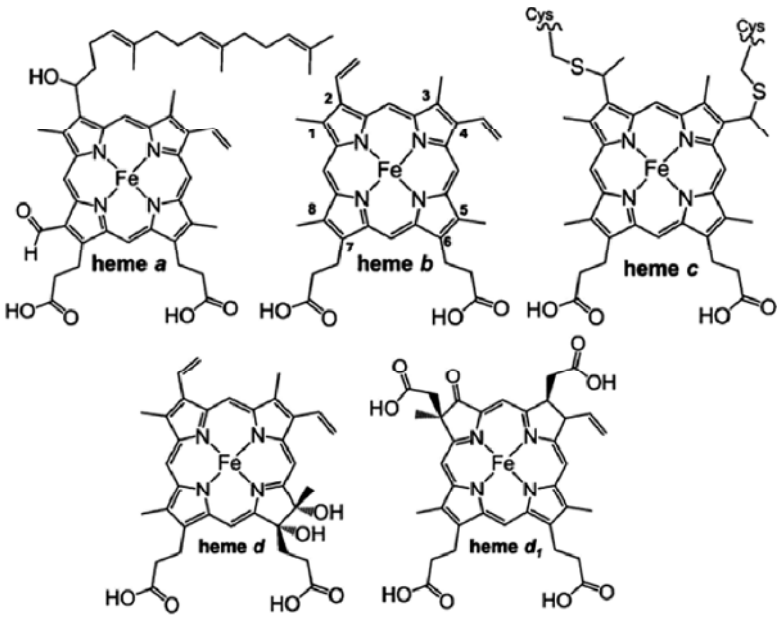

Figure 9 Hemes found in the cytochrome groups. [11]

1.2.1 Biological importance of cytochromes

In mitochondria and chloroplasts the cytochromes mentioned above are often combined to form protein complexes that take part in electron transport and related metabolic pathways. Some of the most notable examples of these combinations will follow in this chapter.

A low spin cytochrome α and a high spin cytochrome α3 are combined to form the subunit III of the cytochrome c oxidase protein complex which is found in eukaryotes and some prokaryotes (Figure 10). This enzyme catalyses the oxidation of mitochondrial cytochrome *c* and some related bacterial proteins, by O_2 [12].

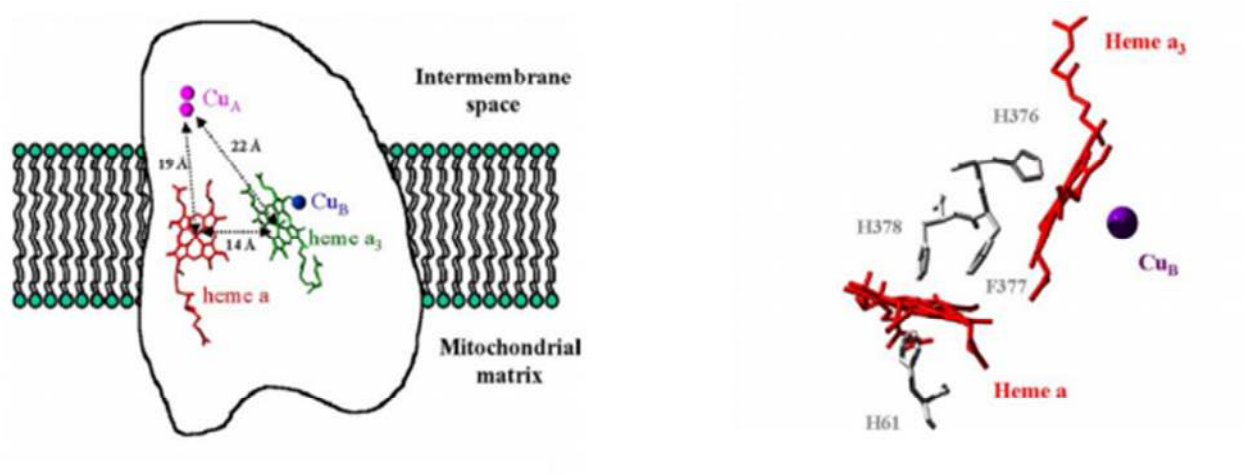

Figure 10 Sketch showing the two heme molecules in cytochrome c oxidase [12]

Cytochrome *b-563*, also known as cytochrome *b6* combined with cytochrome *c*, is found in the *bc1* protein complex. *Bc* complexes are membrane proteins that catalyse the oxidation of ubihydroquinone and the reduction of cytochrome c in mitochondrial respiratory chains and bacterial photosynthetic and respiratory chains. The *bc1* complex operates through a Q-cycle mechanism that combines electron transfer to create a proton gradient, and thus driving ATP synthesis [13].

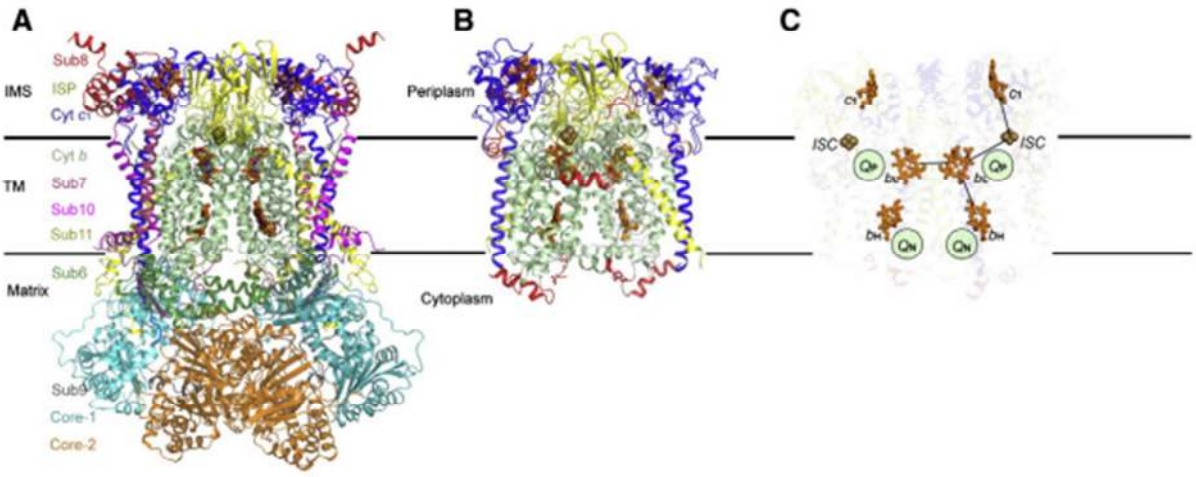

Figure 11 (A) structure of bc1 complex. (B,C) Subunits that take part in Q cycle [13].

Cytochrome *b6* combined with cytochrome *f*, is found in the cytochrome *b6f* complex which links electron transfer between the reaction centres by oxidizing lipophilic plastoquinol and reducing plastocyanin or cytochrome *c6* through a Q cycle (Figures 12,13). [14]

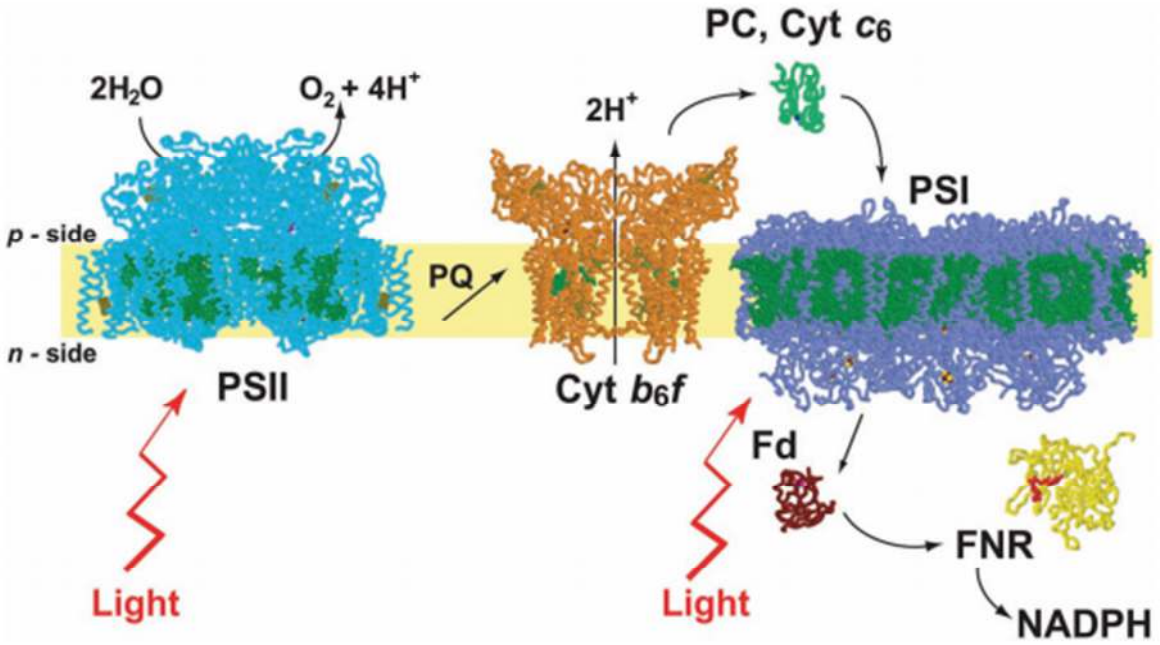

Figure 12 *Cyt b6f* between photosystems I and II . reference

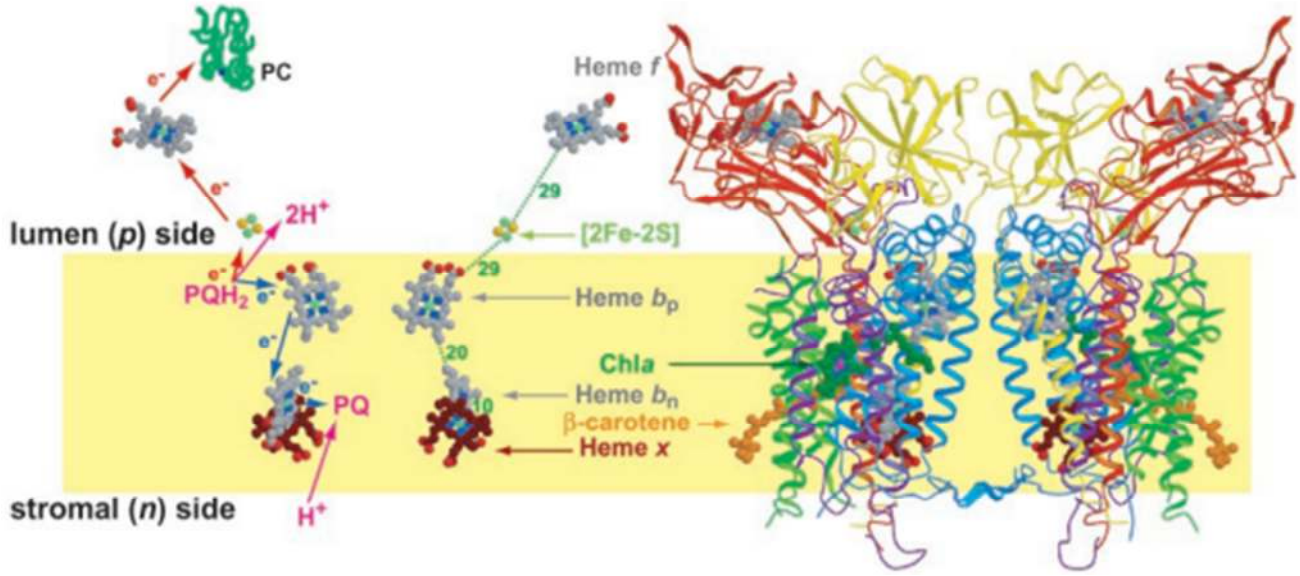

Figure 13 Molecules that take part in b6f Q cycle (Left). Bound co-fcators and protein subunits (Right). [14]

The complexes depicted in Figure 12 and Figure 13, *bc1* and *b6f,* are considered to be homologues with the former functioning in the mitochondrial respiratory chain and the latter functioning in green plant respiratory chains [15]. A comparison of the two is shown in Figure 14

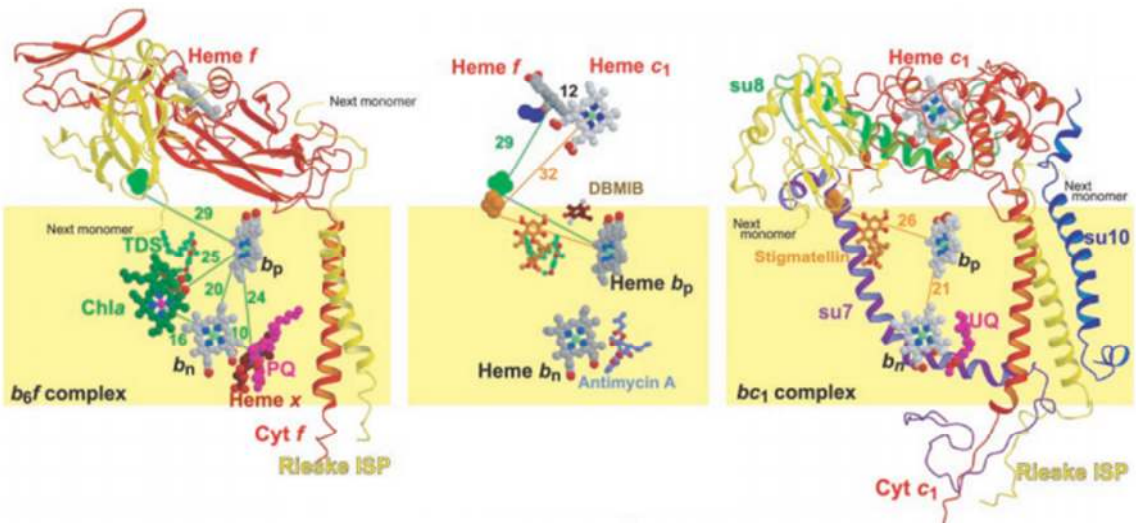

Figure 14 Comparison of b6f (left) and mitochondrial bc1 (right) complex monomers highlighting the positions of *f* and *c1* hemes (center) [14].

Cytochrome *c* can be found in eukaryotic mitochondria where it functions transporting electrons between cytochrome bc_1 complex and cyt *c* oxidase. Although known for its function in the mitochondria, by taking part in the life-supporting function of ATP synthesis, it also plays a vital role in cell death. When an apoptotic signal reaches the cell, cytochrome c is released into the cytosol and triggers programmed cell death through apoptosis [16].

Cytochrome *d*, earlier known as cytochrome/heme a_2 is present in many aerobic bacteria, especially with low oxygen supply. It can be found in *bd-I* terminal oxidase which catalyses the two electron oxidation of ubiquinol and the reduction of O_2 to H_2O. This two-subunit membrane protein (subunits I and II shown in Figure 15) contains three hemes, b_{558}, b_{595} and *d*, and it is generally thought that hemes b_{595} and *d* form a di-heme site for the reduction of O_2 [17].

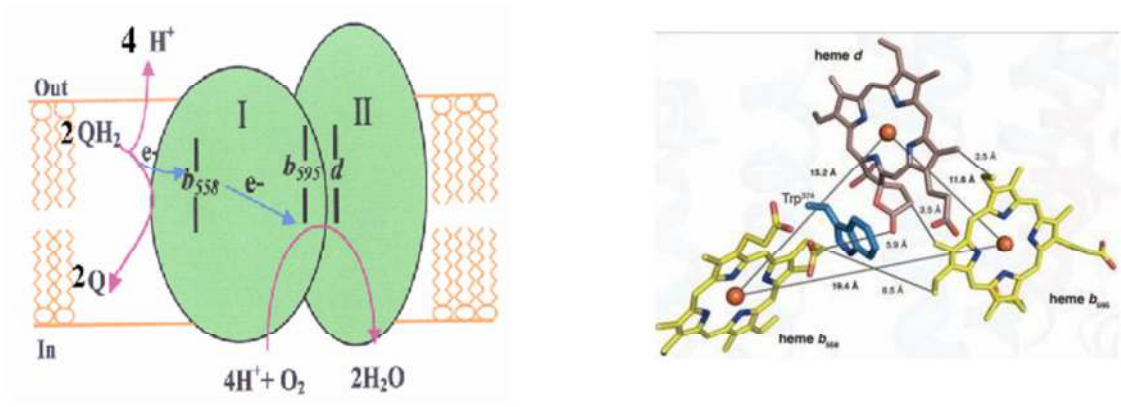

Figure 15 Heme b558 located in subunit I, and heme b595-heme d binuclear center at the interface between subunit I and II. The electron pathway is marked with blue, and proton pathway marked with magenta [18] (Left). Distances between hemes throught crystallographic studies (right) [19].

1.3 Enzyme hemeproteins

1.3.1 Cytochrome p450

The cytochrome P450 enzymes are membrane-bound hemoproteins that contribute in detoxification of xenobiotics, cellular metabolism and homeostasis. They can be activated by xenobiotics and endogenous substrates through receptor-dependent mechanisms and are grouped into two major classes, those involved in the detoxification of xenobiotics, and those involved in the biosynthesis of endogenous compounds. CYP mediated monooxygenation reactions involve embodiment of one oxygen atom into the substrate, while the other is reduced to H_20. [20]

A typical CYP catalysed reaction can be described as follows:

$RH + O_2 + 2e^- + 2H^+ \rightarrow ROH + H_2O$ [14] with the catalytic cycle shown in Figure 16

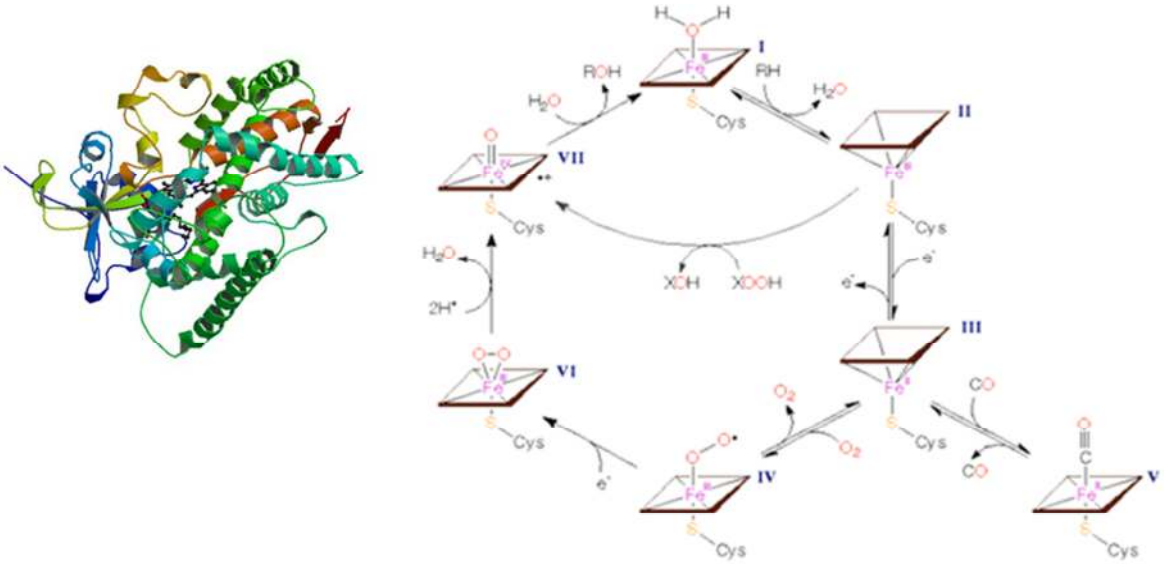

Figure 16 structure[7] (right) and catalytic cycle of *cyt p450* (left). [21]

1.3.2 Catalases and peroxidases

Catalases and peroxidases are antioxidant enzymes that catalyse the decomposition of H_2O_2 to H_2O avoiding free radical formation, thereby protecting the cells from toxic effects of hydrogen peroxide.

$$2H_2O_2 \xrightarrow{catalase} 2H_2O + O_2$$

$$H_2O_2 + AH_2 \xrightarrow{peroxidase} 2H_2O + A$$

Figure 17 Typical reactions that catalases and peroxidases take part in. [22]

Most catalases exist as tetramers of 60 or 75 kDa. They contain four highspin porphyrin heme groups buried deep within their structure, which can be reached through hydrophobic channels that allow the enzyme to react with hydrogen peroxide.[22] According to the structure and sequence, catalases are divided into three classes: monofunctional catalase or typical catalase, catalase-peroxidase, and pseudocatalase or Mn-catalase[23].

Peroxidases, are widely distributed in nature. The heme containing peroxidases have been grouped into two superfamilies, the peroxidase-cyclooxygenase superfamily (PCOXS) and the peroxidase-catalase superfamily (PCATS) (Figure 18). [23]

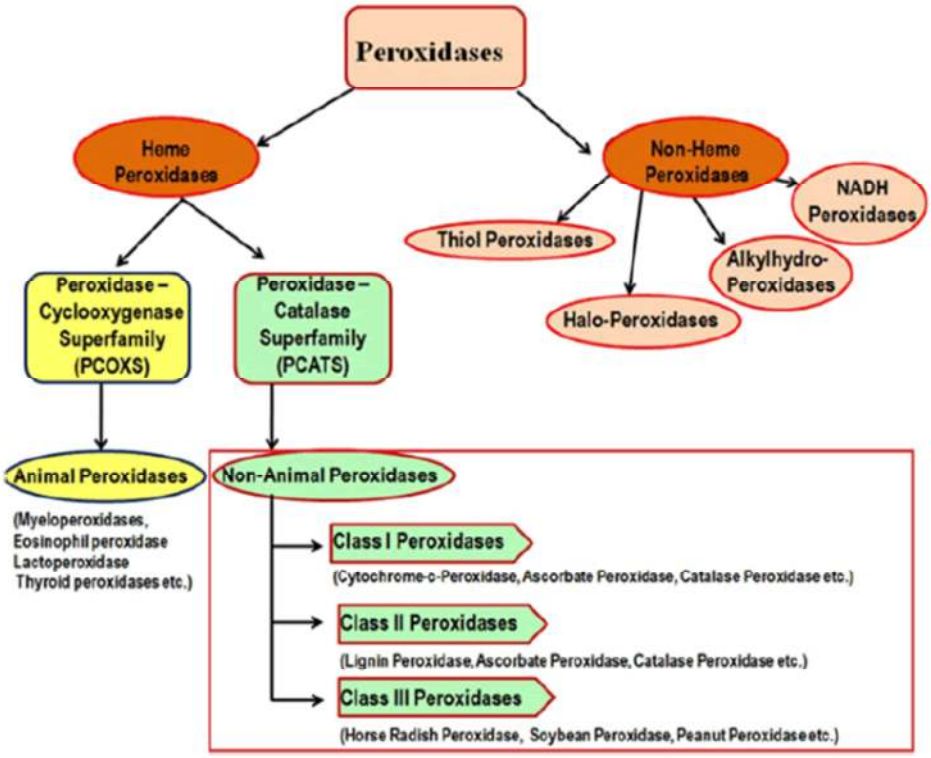

Figure 18 Scheme of the peroxide family. [24]

1.3.3 Lignin-modifying enzymes

Lignin-modifying enzymes (LME) are enzymes produced by fungi and bacteria that catalyse the decomposition of lignin, a biopolymer found in the cell-walls of plants. LMEs include peroxidases, such as lignin peroxidase, manganese peroxidase, versatile peroxidase and many phenol oxidases of the lacasse type. These enzymes belong to the heme-protein family because they carry a protoporphyrin IX as a prosthetic group. [25] The active site which includes the heme group and neighbouring amino acids of one lignin-modyfying enzyme, P.chrysosporium Lip can be seen in Figure 20.

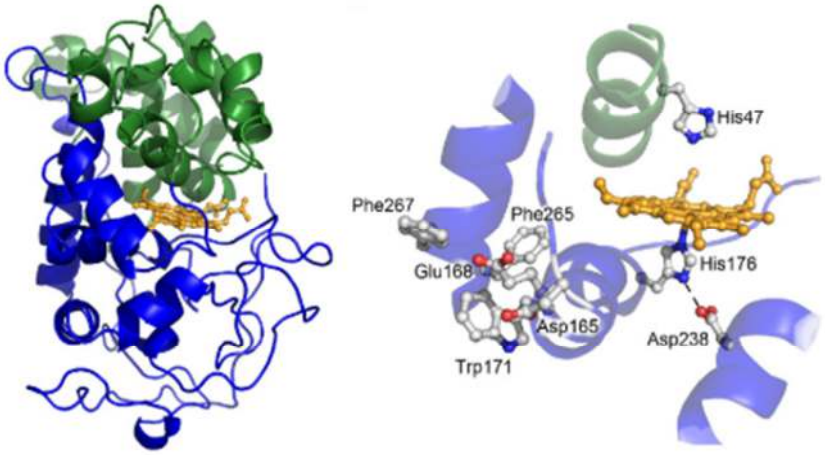

Figure 20 Crystal structure of *P. chrysosporium Lip* [25].

Lignin is a cross-linked macromolecular material derived from oxidative coupling of mono lignols, primarily hydroxycinnamyl alcohols such as p-coumaryl, coniferyl and synapyl alcohols. Lignins exhibit a plant-specific structure, with molecular weight and motif shapes (Figure 21 left) depending on plant species and environmental factors. Lignification occurs by cross-linking reactions of lignin monomers or by polymer–polymer coupling via radicals produced by oxidases. The resonance delocalization of radicals results in various units linked by carbon–carbon and carbon–oxygen (ether) bonds. These bonds mostly include b-O-4, b-5, b-b, 5-5, 5-O-4 and b-1 couplings (Fig 21 right).

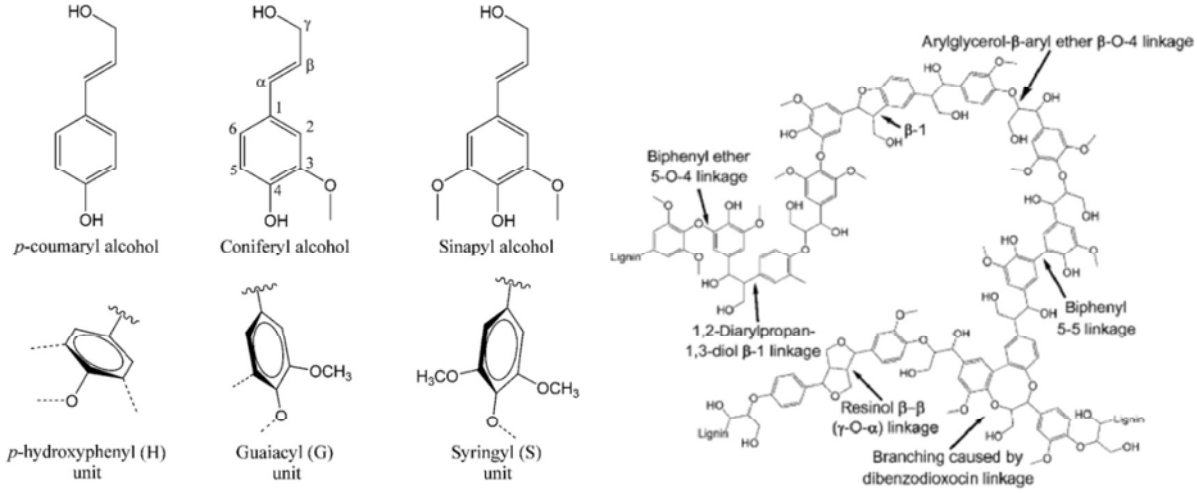

Figure 21 (left) primary lignin monomers, (right) lignin polymer [25].

1.4 Maleimide chemistry

Maleimide and its derivatives are prepared from maleic anhydride by treatment with amines followed by dehydration. A special feature of maleimide is its susceptibility to additions across the double bond by Michael type of mechanisms.

The first step of one of the most widely used maleimide derivative synthesis [27] involves the formation of the sodium salt of amic acid by the reaction of N-phenylmaleamic acid and sodium acetate (Figure 19).

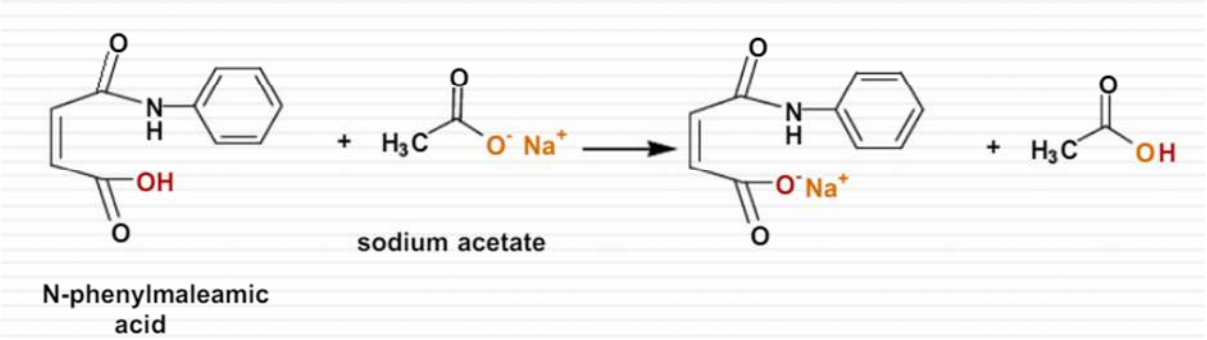

Figure 19[27]

The second step (Figure 20) involves nucleopilic attack of the oxygen anion belonging to the amic acid salt onto the carbon atom of acetic anhydride.

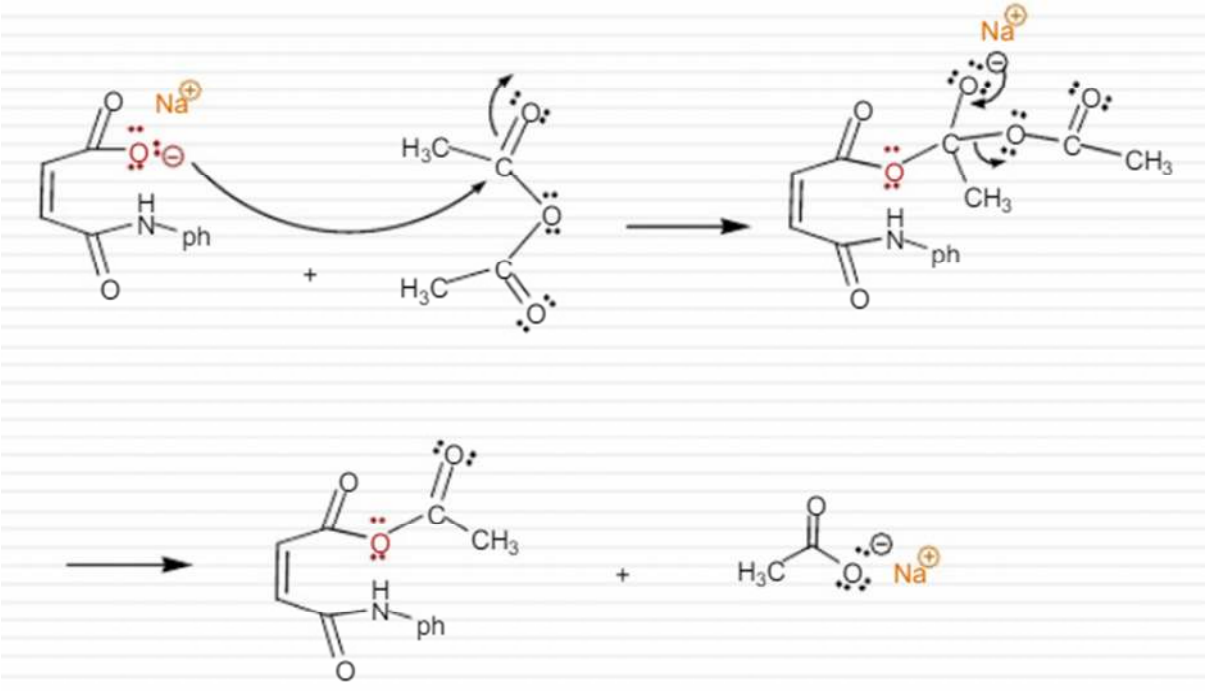

Figure 20[27]

The final step of the maleimide phenyl derivative formation (figure 21) involves a cyclization reaction which takes place between the nitrogen atom the carbonyl resulting in the formation of N-phenylmaleimide.

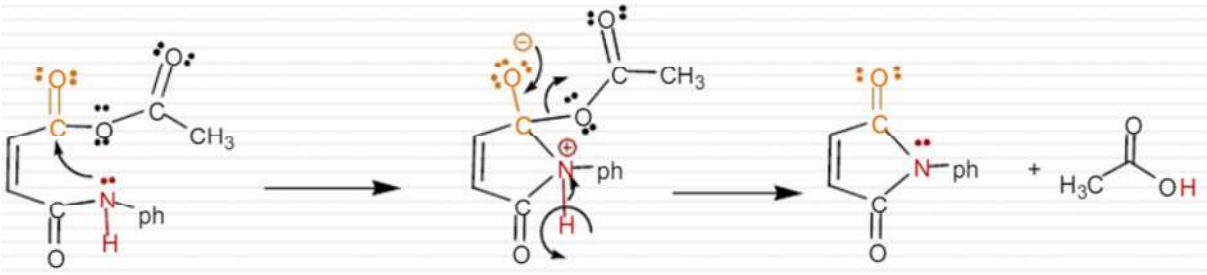

Figure 21[27]

The maleimide group reacts specifically with sulfhydryl groups at a pH range between 6.5 and 7.5 resulting in the formation of stable non reversible thioether bonds (Figure 22). In alkaline conditions, at a pH >8.5, the reaction not only favours primary amines but also increases the hydrolysis rate of the maleimide group resulting in a formation of maleamic acid which cannot further react with thiols (Figure 23). [28]

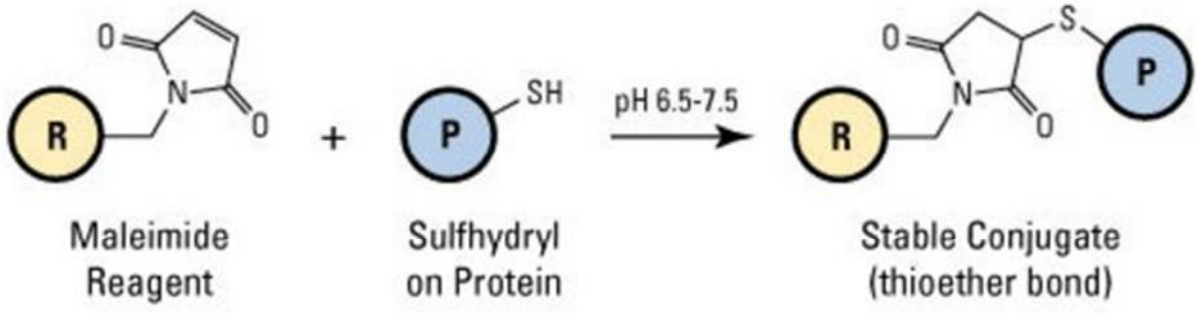

Figure 22 Michael addition of the thiol group on maleimides double bond [28].

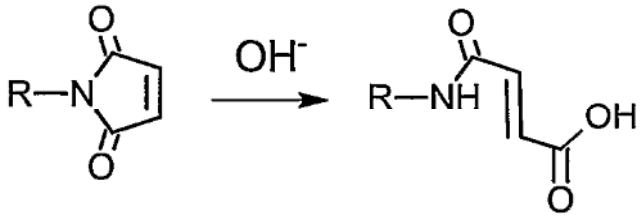

Figure 23 Maleimide hydrolysis under alkaline conditions [29]

1.5 Bioconjugation

Bio conjugation is a strategy for linking molecules together, at least one of which is a biomolecule. Proteins are most notable for bio conjugation due to the wide variety of amino acids and hence suitable substrates for bioconjugations. Moreover proteins can be modified to perform a variety of functions, including cellular tracking, imaging biomarkers, and target drug delivery.

Classical protein bioconjugation reactions target side chains of certain amino acids such as cysteine and lysine. The table below shows reactions including these amino acids [30]

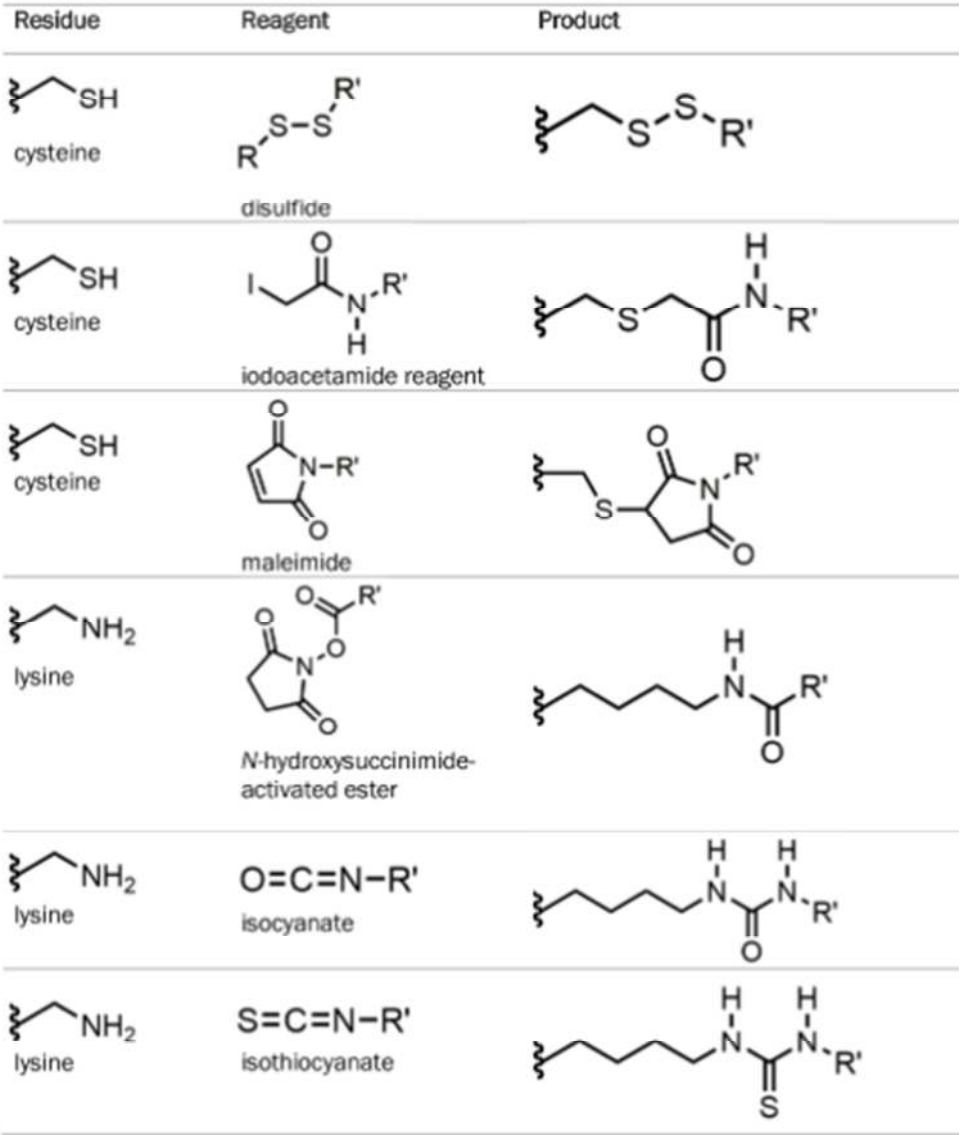

Figure 24 classical approach for protein bioconjugates [30]

Porphyrin boconjugation strategy depends on the functional group. 3 major reaction groups are depicted in Figure 25. Ligations based on bioorthogonal (1) reaction which included Husgen reaction, Staudinger ligation and metathesis reaction, thiol targeting reactions (2) which include thiol/maleimide reactions and thiol/haloacetamide ligation and amino-carboxy targeting reactions (3) which include thiurea and amide formations.

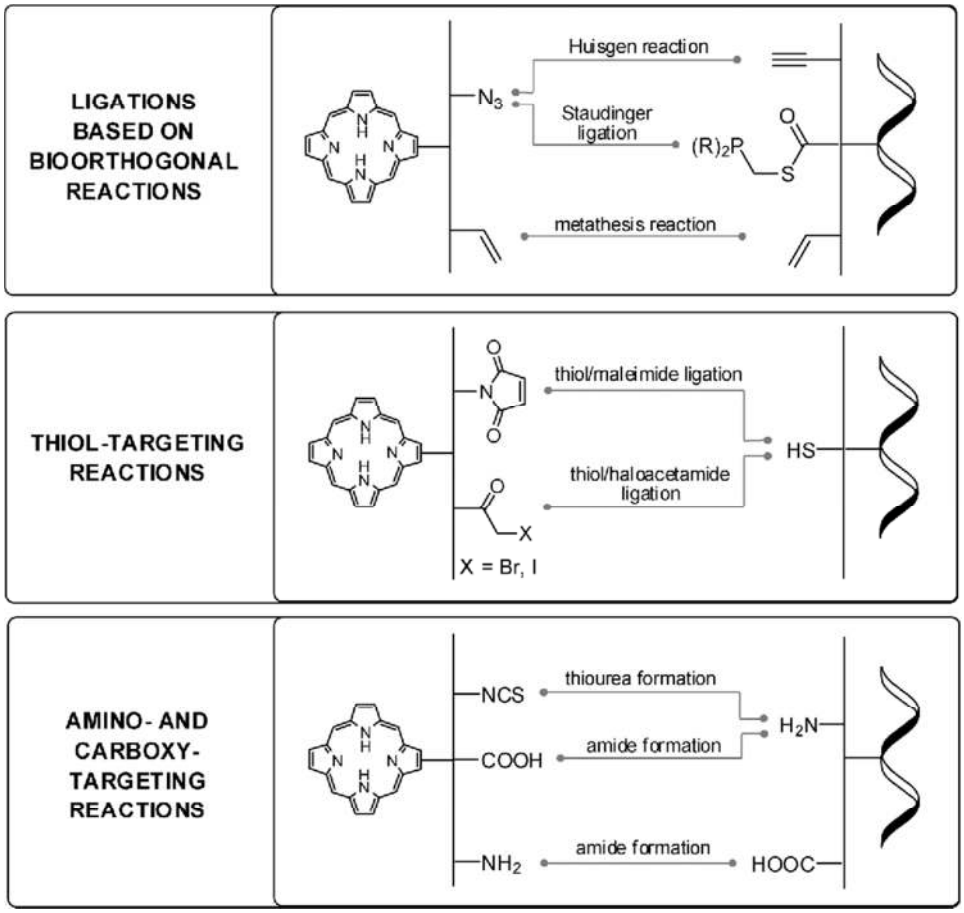

Figure 25 Porphyrin conjugation reactions [41]

1.6 Purpose of thesis

As mentioned above, the main purpose of the thesis was the synthesis of hybrid protein-porphyrin chimeras i.e. to create a hybrid hemeprotein. In doing this we could study whether or not we could introduce catalytic properties to a protein and also check if enhance stereo selectivity could be achieved. Furthermore, if successful we could set up experimental procedures leading to multi-functionlized protein hybrids.

The first step of this project involved the synthesis of a porphyrin–maleimide derivative which would then be grafted onto a protein through maleimide coupling (Figure 26). The latter steps of the project involved iron metalation of the porphyrin derivative and subsequently study of the catalytic properties of the synthesized chimera.

In this thesis, the widely used, commercially available protein BSA was used as a model protein since it bears one free thiol group at Cys34 residue which is ideal for maleimide coupling. A tetraphenyl-porpphyrin-maleimide derivative was synthesized and covalently linked to the protein.

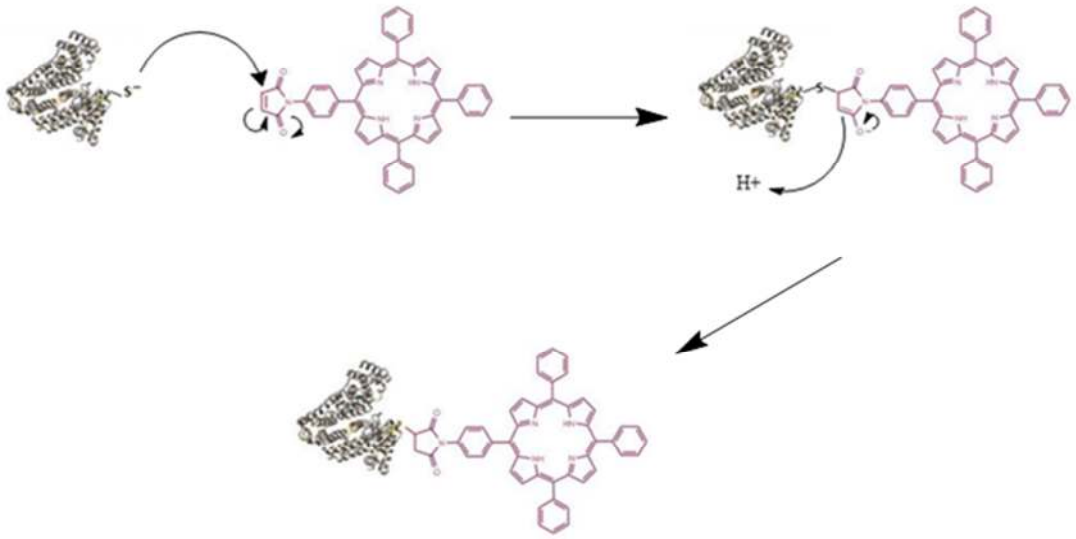

Figure 26 Schematic representation of the synthetic approach involving a Michael addition between the thiol group of BSA and maleimide group of the porphyrin

2.0 Results and discussion

Synthesis of Porphyrin-maleimide derivative

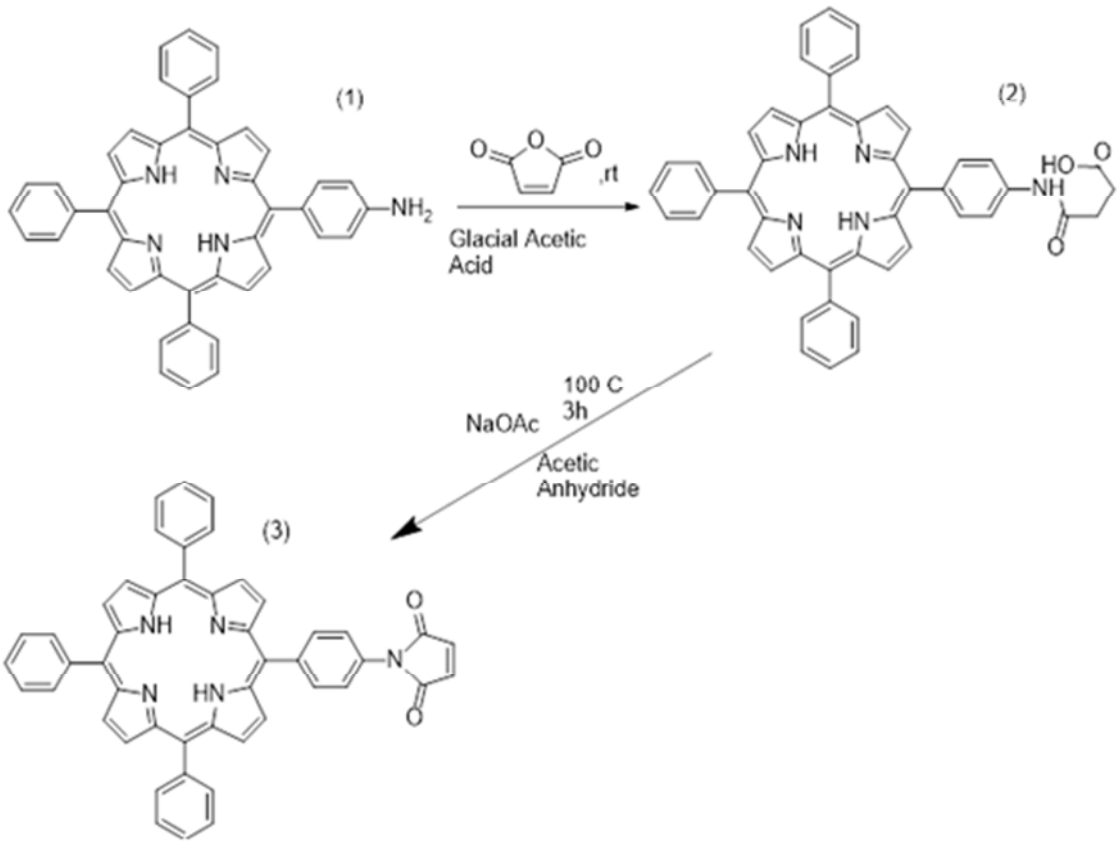

Figure 27 Synthetic pathway for the porphyrin-maleimide derivative [38]

For the synthesis of the the porphyrin maleimide derivative, tetraphenyl porphyrin (1) and an excess amount of maleic acid were added to glacial acetic acid to form the intermediate derivative (2). The excess amount of maleic acid was added to ensure increased yield of the intermediate (2). The glacial acetic acid was used to create anhydrous conditions during the synthesis. Addition of NaOAc and acetic anhydride to the intermediate (2) at 100 ^{o}C led to the formation of the maleimide porphyrin derivative (3) after 3 hours through the mechanisms shown in maleimide chemistry chapter. Following the above synthetic protocol, the product was purified via column chromatography initially using DCM (99% purity):Hexane 9:1 as an eluent and then once clear band separation was observed, the elution solvent polarity was slightly increased to DCM (99% purity).The increase in polarity assisted in eluting the product faster since at that point it was the only compound adsorbed in the column as indicated. Thin Layer Chromatography (TLC). TLC also indicated that DCM (99% purity): Hexane 9:1 was a suitable solvent for separation.

Figure 28 Virtual representation of the TLC plate after synthesis of porphyrin maleimide derivative (3).

TLC using DCM (99%): Hexane 9:1 showed a good separation of the 2 spots, one shown in green and one shown in a maroon shade (Rf was not measured as we were interested in optical separation of the 2 spots.) with the green spot corresponding to either a protonated porphyrin form formed due to the the acidic environment and not fully neutralized after the addition of NaOAc, or a by-product often found in porphyrin synthesis called clorin. The maroon spot corresponds to the maleimide-porphyrin free base.

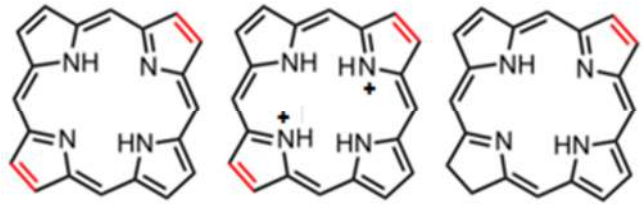

Figure 29 (Left) Porphyrin free base, (Center) Protonated porphyrin, (Right) Clorin

Figure 30 Column chromatography separation of the porphyrin maleimide product (3) after depletion of the green by-product band

The chromatographic separation was initiated with DCM: Hexane 9:1 as an eluent based on TLC. Once the depletion of the green band was achieved as shown in Figure 30, the polarity was increased to DCM (99% purity) to speed up product elution.

MALDI-TOF results indicate at the formation of a relatively clean product. Since it was known that this synthetic approach was successful according to the work of Kostas Karikis[41], it was decided to continue characterization with MALDI TOFF which would identify impurities in the product mixture instead of NMR.

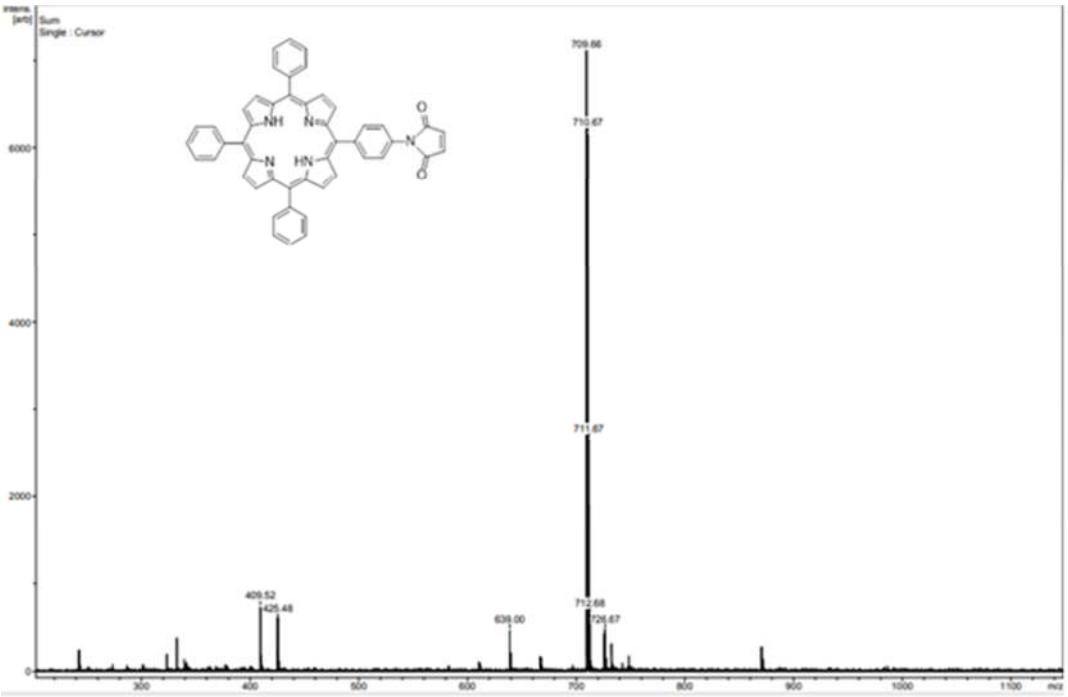

Figure 31 MALDI-TOFF studies of maleimide porphyrin derivative

The peak at 400 m/z corresponds to the matrix used. The peak at 629 m/z corresponds to unreacted tetraphenyl porphyrin and the peak at 728 m/z corresponds to a product in which the maleimide ring has been hydrolysed hence having a MW of plus 18.

UV-VIS studies were performed on the product to investigate the wavelength of the Soret band which is a characteristic band that porphyrins exhibit around 420nm (Figure 31). The origin of Soret bands is due to S0- S2 transitions. The Soret band of the maleimide derivative appeared at 419nm. The 4 bands of smaller intensity that appear in the spectra are called Q bands and arise from S0-S1 transitions (Figure 30).

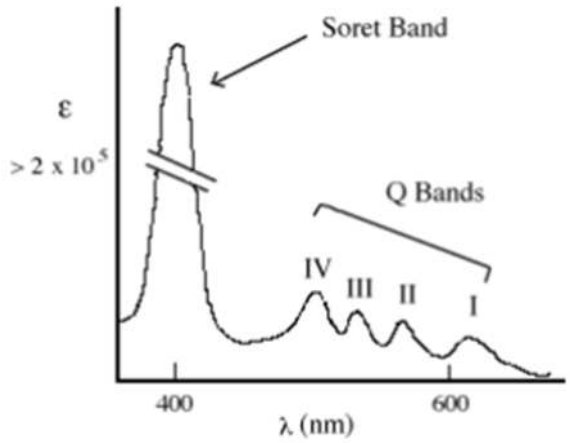

Figure 32 Typical porphyrin UV-Vis spectra bands[31]

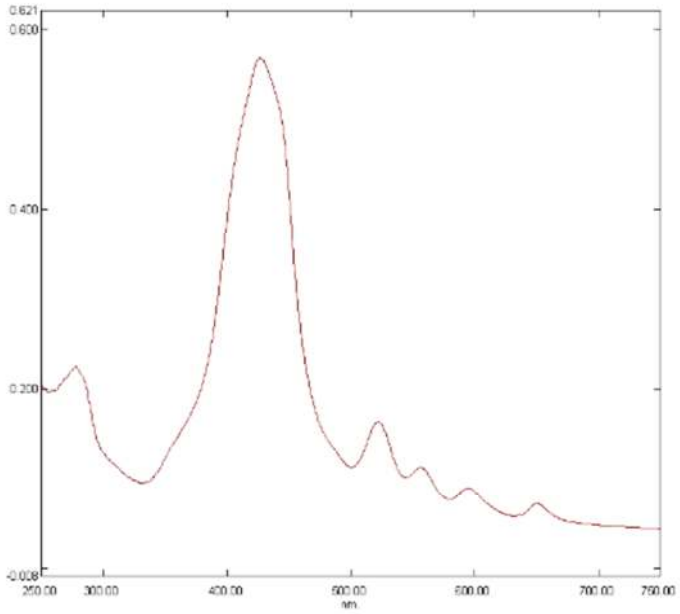

Figure 33 UV-Vis spectrum of the maleimide-porphyrin product (3) with a Soret band at 419 nm

Synthesis of the BSA-porphyrin chimera

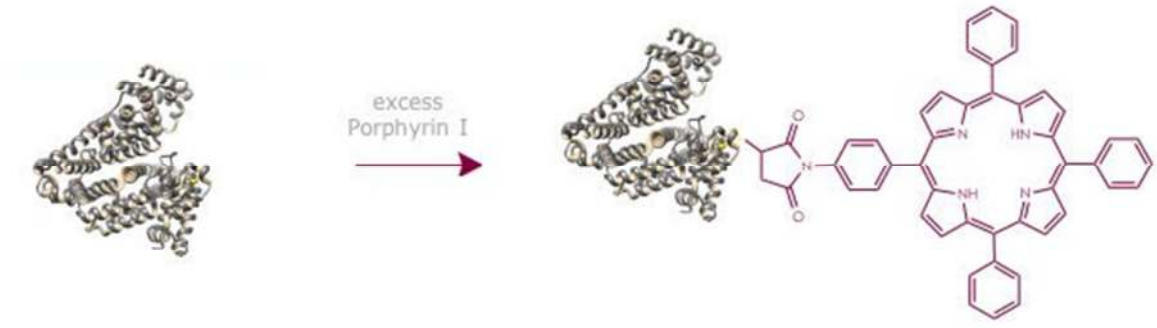

Figure 34 Synthetic approach followed for the BSA-porphyrin chimera.

For the synthesis of the BSA-porphyrin chimera an excess of the maleimide-porphyrin derivative (3) in DMSO was added to a protein buffered solution (pH=7.4) and left to gently shake for 48 hours at RT. The DMSO to buffer ratio used was 1:10 in order to ensure that the protein is kept in a stable environment. The excess of the maleimide-porphyrin derivative was required to increase the collision rate which would accelerate the reaction completion.

In regards to maleimide chemistry, it has been previously shown that use of a large excess of the maleimide derivative (1:30 ratio) is necessary to insure an adequate yield and simplify isolation protocols.[32] When the bioconjugation reaction was performed using a maleimide to thiol excess of 1:30 it led to a relatively small yield according to GPC results. More specifically, as shown in Figure 35, we see that BSA's elution time measuring at 254 nm (where amino acids strongly absorb) is approximately 12-13 minutes. The reaction product (orange curve) exhibits a bimodal elution pattern, with the first peak at the 10 minute mark and the second at 12-13 minutes. The peak at 12-13 minutes for the product matches with BSA's lone peak so we can attribute it to unreacted BSA. The peak at 10 minutes can be attributed to a product with larger molecular weight than BSA due to its shorter elution time. We assumed that this was the mono-bioconjugate and performed another GPC measurement, this time at 410 nm, a region where porphyrins exhibit strong absorbance (Soret region). Since porphyrins are molecules of small molecular weight their elution could only be monitored after the separation limit of ~20 minutes, but the much larger porphyrin derivative i.e. the protein-porphyrin product would be expected to elute with a retention time shorter than that of BSA. The purple curve depicting the measurement at 410 nm showed firstly no peaks at 12-13 minutes which was expected as proteins do not absorb at 410 nm and secondly a peak with elution time that matches the elution time of the product measured at 254 nm which confirming that this peak corresponds to a single product containing both a protein and a porphyrin, i.e. the targeted bioconjugate. When the experiment was repeated using increased maleimide to thiol ratios, we concluded that a 1:90 thiol to maleimide ratio excess produced the best results (figure 36).

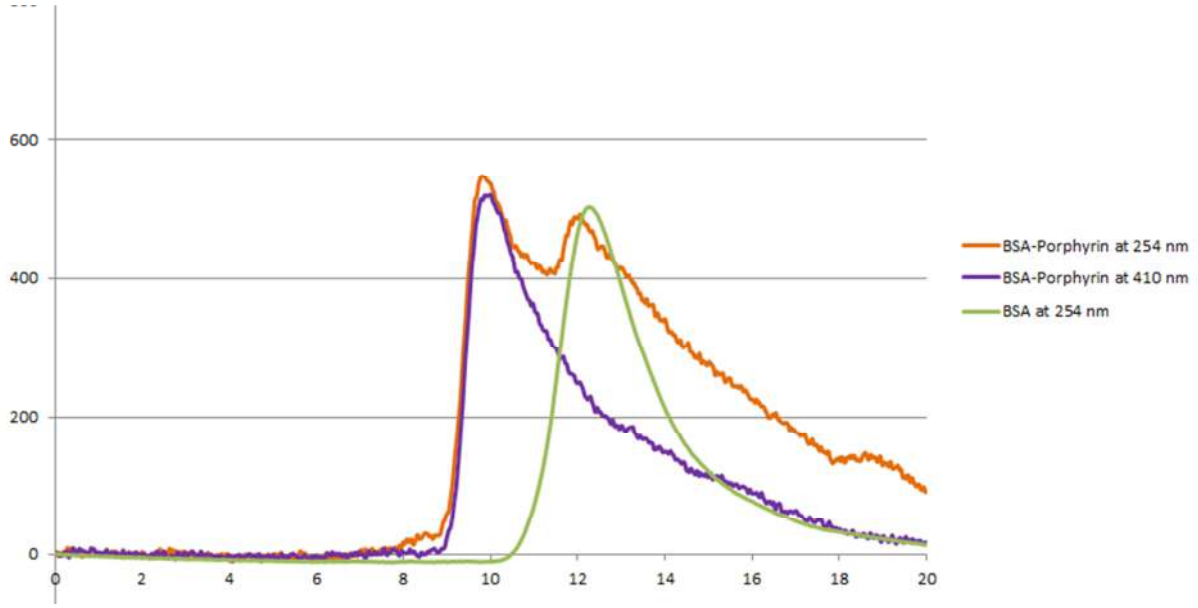

Figure 35 GPC results of BSA-porphyrin chimera using a 1:30 ratio measured at both 254 and 410 nm.

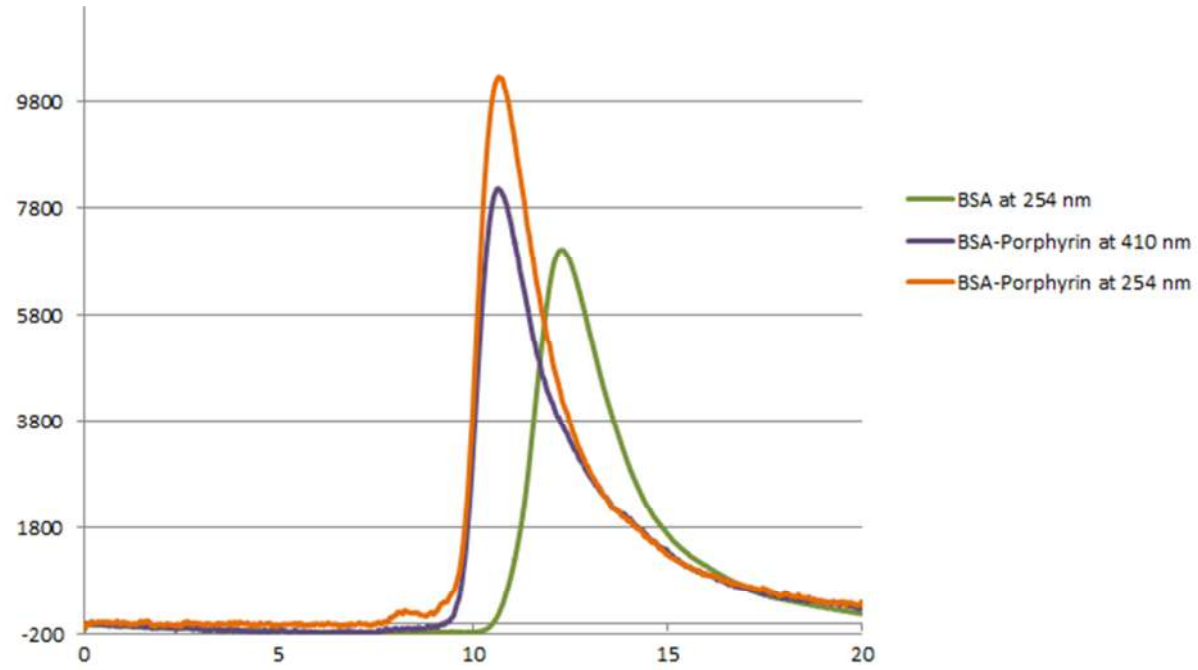

Figure 36 GPC results of BSA-porphyrin chimera using a 1:90 ratio measured at both 254 and 410 nm.

Analysis with MALDI-TOF MS of the 1:90 ratio product indicated at the formation of a new species with mass at 67311m/z (Figure 37). The product differs 725 m/z for the native protein BSA measured at 66856 m/z (Figure 36). This approximately corresponds to the molecular weight of the porphyrin maleimide derivative (709 m/z) leading to the conclusion

that the targeted monoadduct was synthesized. MALDI is therefore consistent with the GPC studies (Figure 36) and proves the formation of the monoadduct BSA-porphyrin II.

It should be noted that many attempts were made at MALDI analysis but no results could be initially obtained. For this reason, to obtain the optimum result presented above, the focus was shifted to both synthesis optimization and sample preparation. For synthesis optimization, reactions with variable porphyrin to protein ratios were performed and then analysed -only the successful final attempt was analysed in this manuscript. Further optimization attempts were focused on adding different detergents, such as SDS and TWEEN, to the reaction mixtures to aid the porphyrin conjugation. Unfortunately MALDI did not show any results. The focus was then shifted to matrix variations. Since the matrix is the substance added to aid sample ionization, it was thought that matrix variation could give further insight. Four different matrices were used (namely, a-cyano, Super DHB, sinapic acid, dithranol) with unclear results. Having gathered no solid results, it was decided to prepare fresh matrices and measure immediately after preparation. Out of the four matrices, a-cyano was the only matrix to produce a clear result (Figure 37). Super DHB still gave unclear results depicting a wrong m/z while the other two matrices (sinapic acid and dithranol) gave no results.

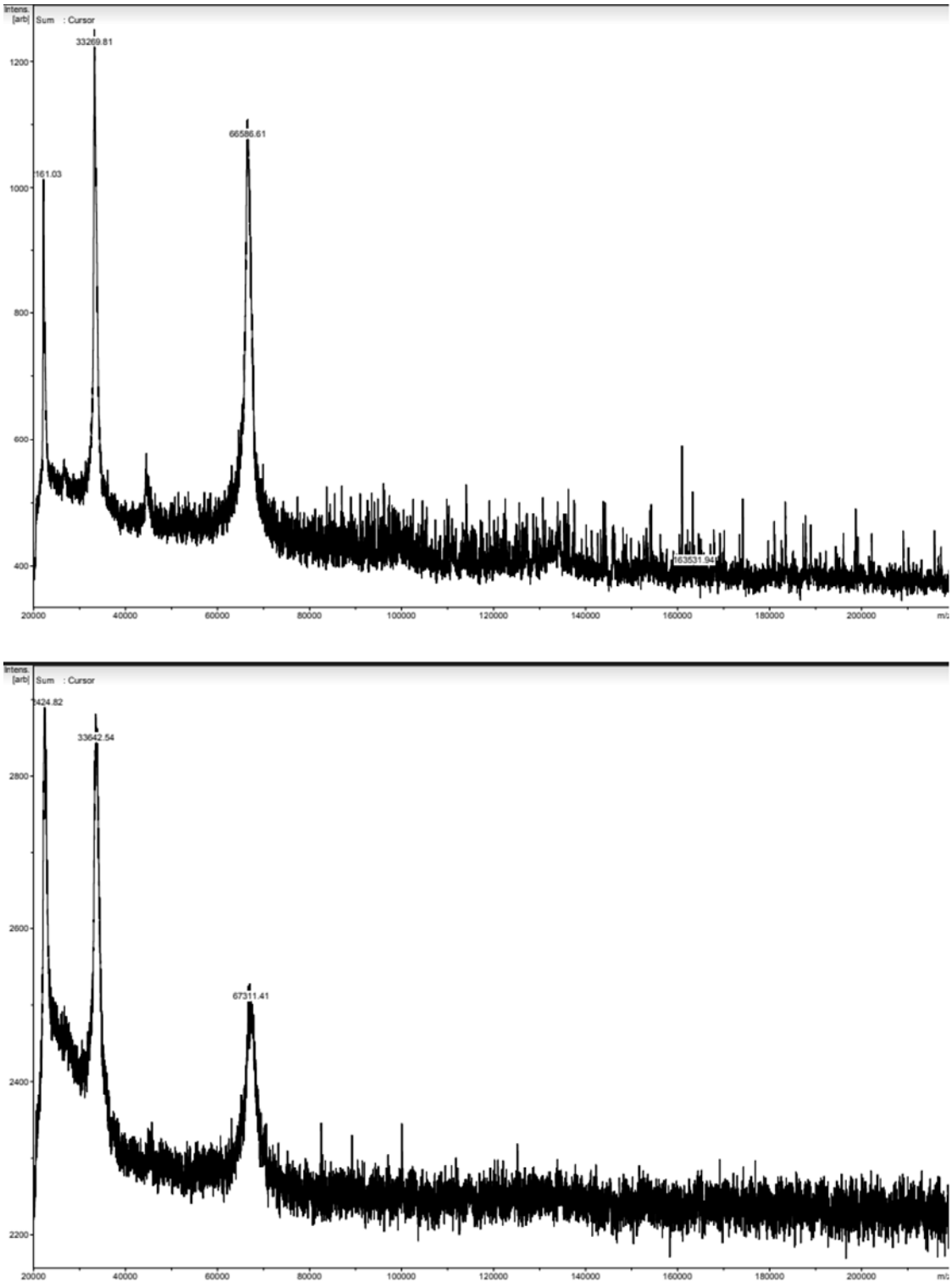

Figure 37 (top) MALDI-TOF spectrum of BSA and (below) Porphyrin conjugated protein

The product was also analysed with ESI MS. Sample preparation included the addition of ethanol which would denature the protein and acetic acid which would charge the protein molecules. Denaturation would in principle aid homogenous charge distribution of the protein. We were unable to get a clear and thus correct spectrum of BSA (Figure 38, while the spectrum of BSA-porphyrin could not be obtained using the software. It remains unclear

to which degree sample treatment could be at fault, but due to the lack of information provided by this technique we decided not to investigate further.

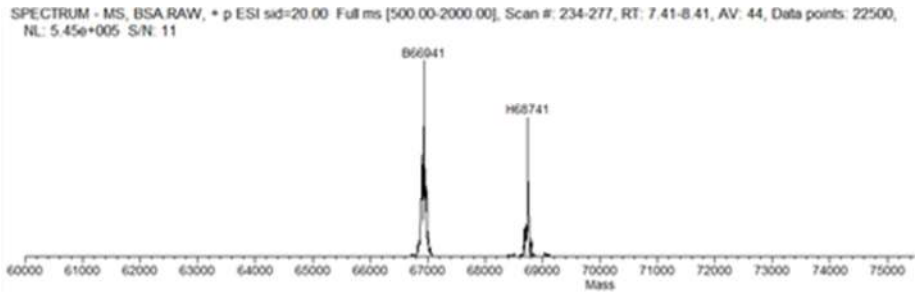

Figure 38 ESI-MS spectrum of BSA

IR studies were also performed (Figure 40). The goal was to identify BSA's free thiol group (2540-2600 cm^{-1}) and study whether we could monitor its disappearance in the product, to investigate whether the peak that corresponds to maleimide's double bond appears in the product[33] (1630 cm^{-1}) and lastly to investigate the whether a peak corresponding to the C-S-C [34] bond formation appears in the product (750 cm^{-1}) (orange bonds in Figure 39). All bond vibrations under investigation are shown in Figure 39 in orange colour. Unfortunately, there are several limitations to this approach which include the weak absorbance of thiol groups therefore a peak was not visible, a failure to achieve depletion of excess unreacted porphyrin-maleimide derivative following the chimera synthesis therefore malemide's double bond still appeared in the spectrum and lastly the newly formed C-S-C bond is also present in methionine, an amino acid found 5 times in BSA. Because of the lack of information obtained we decided not to investigate any further the progress of the reaction via IR.

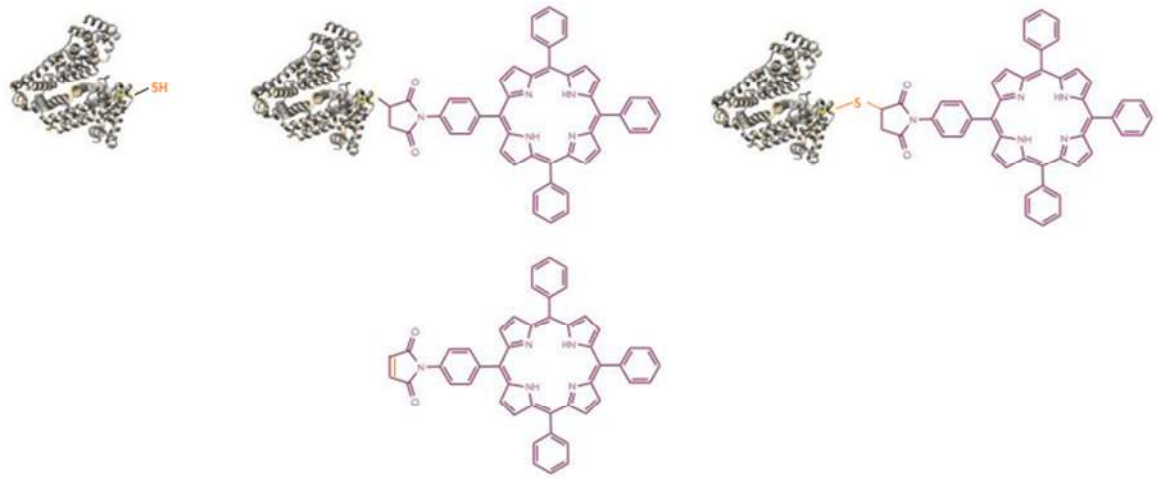

Figure 39 Bonds (in orange) targeted via IR spectroscopy. (left) free thiol group, (center) maleimide's double bond, (right) c-s-c bond

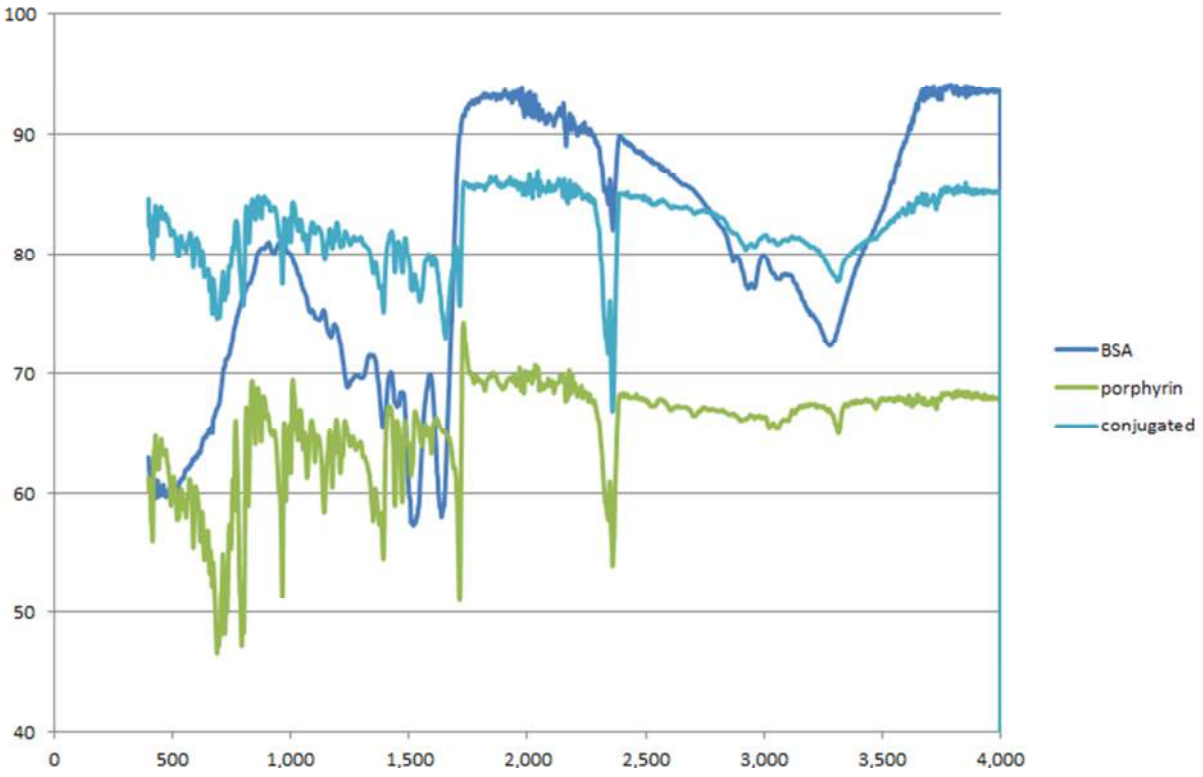

Figure 40 IR spectrum of (top) BSA, (middle) porphyrin conjucated protein and (bottom) maleimide-porphyrin derivative

SDS PAGE electrophoresis performed on the product (Figure 41) did not provide any indication via the formation of a new band for the product as the bands of (a) BSA and (b) BSA-Porphyrin exhibited an overall zero net mobility change. This could be interpreted as a change in BSA's tertiary structure and charge upon porphyrin conjugation leading to both a molecular weight increase and a molecular shape distortion.

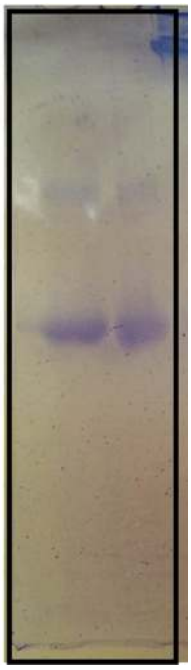

Figure 41 SDS-PAGE electrophoresis gel results of (left) BSA and (right) porphyrin conjugated protein.

Laemmli SDS PAGE electrophoresis was also performed (Figure 42) for samples of a larger concentration in order to observe if the band attributed to the product would present fluorescence under UV light due to the presence of porphyrin. Since the product was visualized as a brown band (with migration same as BSA) before staining, fluorescence was not necessary. One limitation of this method however was that in order to conduct Laemmli SDS PAGE electrophoresis, the sample was first heated followed by an addition of beta mercaptoethanol acting as a reducing agent. It is possible that the coloured band could be the result of a conjugation at a newly formed thiol group via S-S bridge reduction. Because of this potential limitation, we treat these results with caution.

Figure 42 Laemmli SDS-PAGE gel results of porphyrin conjugated protein. A dim-light brown band can be seen within the black lines.

Synthesis of poly-conjugated biohybrid

An attempt was made to synthesise polyconjugated biohybrids by reducing disulphide bonds which would free up SH groups. BSA contains 17 disulphide bonds (at positions 77-86, 99-115, 114-125, 147-192, 191-200, 223-269, 268-276, 288-302, 301-312, 339-384, 383-392, 415-461, 460-471, 484-500, 499-510, 537-582).[35]

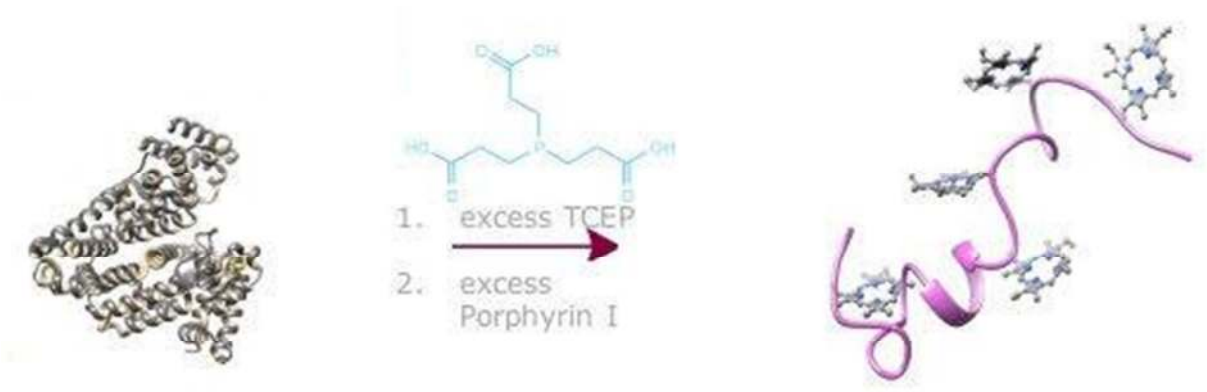

Figure 43 Schematic representation of the synthetic approach used for the synthesis of poly-conjugated biohybrids.

For the synthesis of polyconjugated biohybrids, an excess of reducing agent TCEP as well as an excess of maleimide-porphyrin derivative was required. Starting with an aqueous protein solution TCEP was added and left to gently shake at room temperature for 30 minutes. According to literature,[36] using 34 equivalents of TCEP (2 per S-S) should secure the complete reduction of the protein moiety. A maleimide-porphyrin solution in DMSO was then slowly added to the aqueous solution and left to shake at room temperature for 48 hours. Due to the excess amount of porphyrin used, it was necessary to use a larger amount

of DMSO to achieve dissolution. It was judged that for this study the aqueous to organic solvent ratio was not important, as it was in the synthesis of the mono adduct, because the protein was denatured via S-S bridge reduction.

Attempts to quantify free thiol groups were performed using Ellman's reagent to verify the complete reduction of disulphide bridges. DTNB (Ellman's reagent) reacts with a free sulfhydryl group to yield a mixed disulphide and 2-nitro-5-thiobenzoic acid (TNB yellow colour, Figure 43). The target of DTNB in this reaction is the conjugate base ($R—S^-$) of a free sulfhydryl group. Sulfhydryl groups may be estimated in a sample by comparison to a standard curve constructed from known concentrations of a sulfhydryl-containing compound such as cysteine.[37]

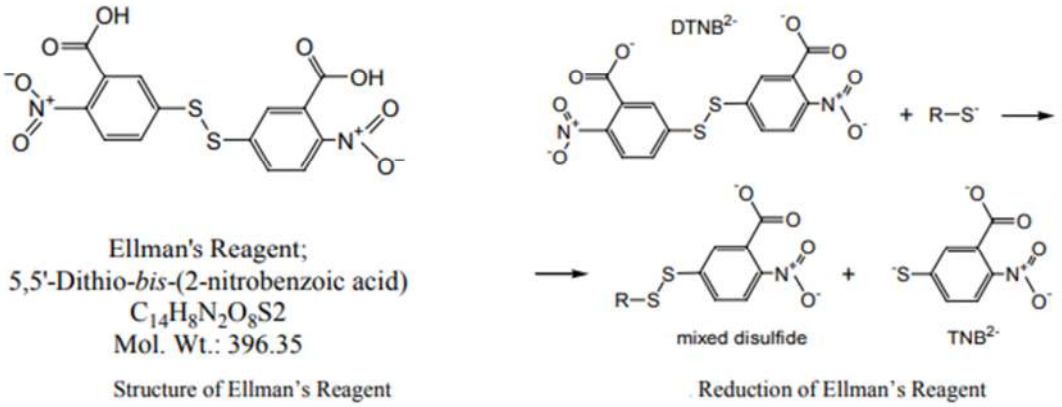

Figure 43 Ellman's assay reaction

For the Ellman's assay, a standard curve was created using l-cysteine as a thiol source. After the standard curve plot, 2 sample solutions were measured, first was a 0.3 mM native BSA solution which yielded a 0.6 absorbance and second was a 0.3 mM BSA solution that had been treated with 1:1 TCEP yielding a 0.18 absorbance. At a first glance these values seem logical due to the fact that TCEP reduces a disulphide bridge exposing 2 free thiols which means that the overall thiol concentration of the second sample would be 3 times larger (1 free thiol vs 3 free thiols) than that of the first sample (Figure 44).

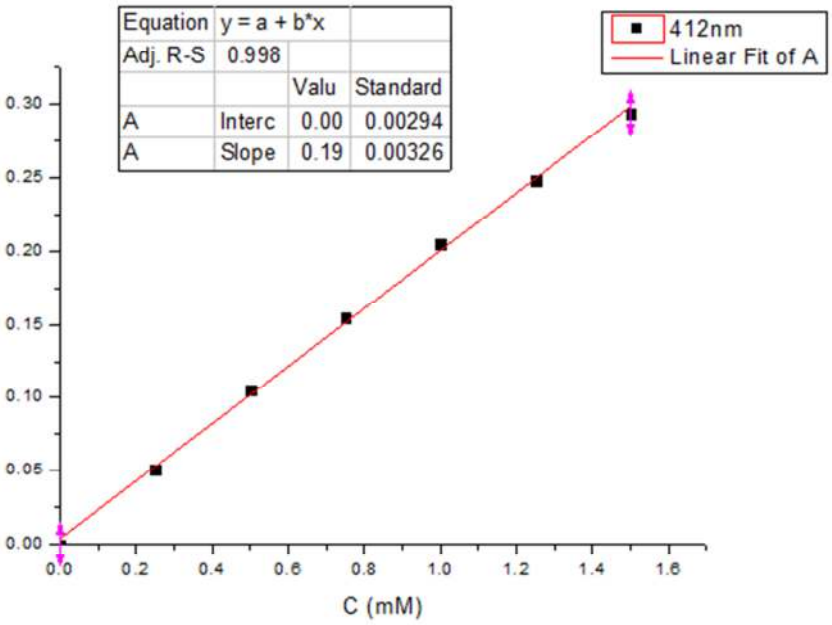

C	A
mM	
	412nm
1.5	0.294
1.25	0.248
1	0.205
0.75	0.155
0.5	0.106
0.25	0.051
0	0

Figure 43 Ellman's assay on reduced protein

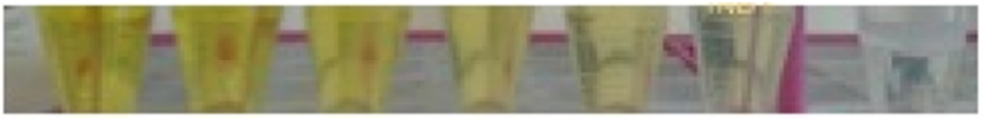

Figure 44 Visual representation on Ellman's reagent assay with standard curve concentrations starting from high to low

Although Ellman's assay quantifies free SH concentration, a blank experiment with just Ellman's reagent and TCEP revealed a reaction between the reagents due to the fact that TCEP can also reduce the disulphide bridge of the Ellman's reagent.

In order for a reliable Ellmans assay, we must assure that all the TCEP has reacted quantitatively with S-S bridges before adding the DTNB reagent, else there is a possibility of TCEP reducing the S-S bridge within DTNB resulting in false information. Perhaps experiment replications with a variable reaction time between TCEP and Protein S-S bridges could give a clear insight.

Analysis of the polyconjugated sample was with GPC (Figure 45) showed that the elution times of sample and BSA indeed differ, however, when comparing our results to those of the mono-conjugated we notice that their elution times match (both at the 10 minute mark), which is a very unlikely outcome. Such behaviour remains unknown although an argument could be that Figure 45 below depicts the non-reduced mono-conjugated adduct and the poly-conjugated product does not elute from the column.

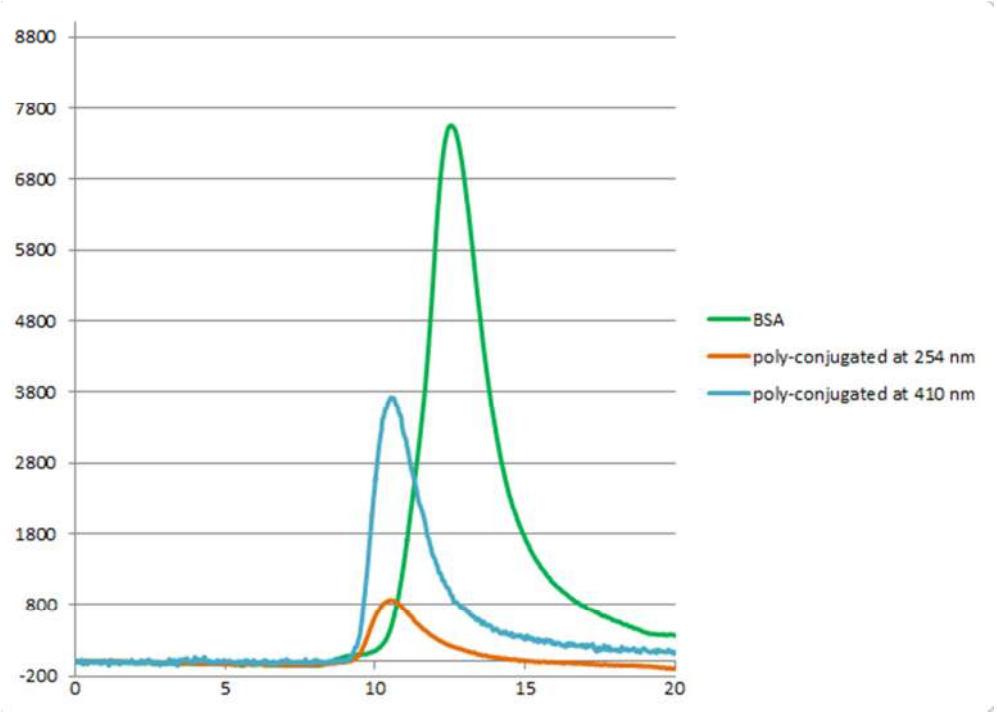

Figure 45 GPC chromatography results of (green) BSA, (orange) polyconjugated product at 254 nm and (blue) polyconjugated product at 410 nm.

MALDI TOF MS did not provide useful results. A very noisy spectrum was recorded. SDS PAGE electrophoresis was also performed on the sample (Figure 46). A broad band was observed which could be considered as different conjugated protein moieties, supporting conjugation. Due to the amount of data obtained during the characterization and its clarity, we treat these findings with caution.

Figure 46 SDS-PAGE results of (left) poly-conjucated porphyrin-protein chimera and (right) BSA.

Fe-metalated monoamino-tetraphenylporphyrin

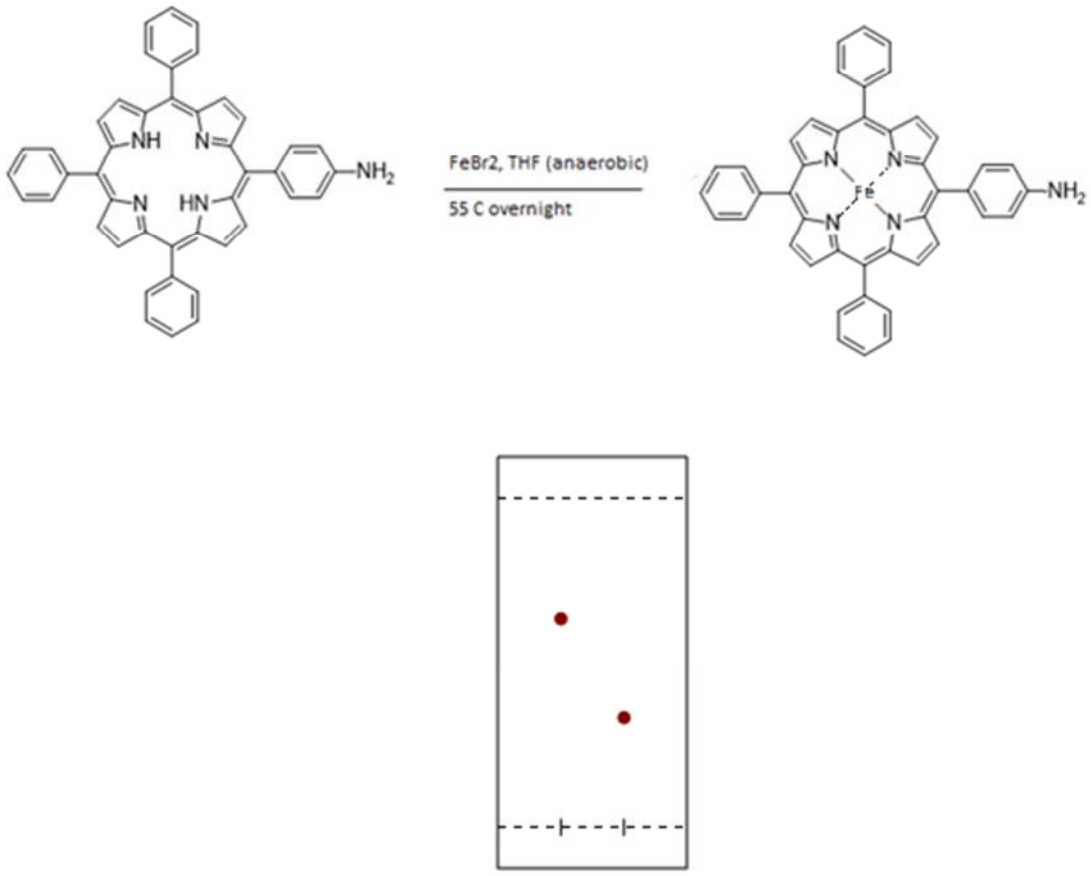

Figure 47 Synthesis of the Fe-metalated monoamino tetraphenyl porphyrin (top), TLC chromatography (bottom) (Left) Non matalated porphyrin, (Right) metalated porphyrin

For the synthesis of Fe-metalated monoamino tetraphenyl porphyrin, monoamino tetraphenyl porphyrin and $FeBr_2$ were added to dry THF and stirred overnight at 55 ^{o}C under anaerobic conditions. The anaerobic conditions were necessary to avoid oxidation of Fe^{2+} to Fe^{3+} under oxygen. Following the above synthesis, a TLC was performed which was expected to indicate product formation. The presence of Fe ion in the porphyrin ring increases the compounds' polarity therefore the product will not migrate as far as the non-metalated porphyrin on TLC. The separating solvent chosen for TLC was DCM: MeOH 99.9 :0.1.

After purification by column chromatography, the eluted band containing the desired product was analysed with MALDI TOFF. From the spectrum (Figure 48) we could see that complete separation of the metalated product from the non metalated product wasnot be accomplished despite the fact that the sample was purified twice in an effort to obtain a pure product. We decided to continue with the synthesis of the maleimide product with a lightly contaminated reactant as a third column would result in a relative significant loss of product. The monoamino-porphyrin was therefore used for the synthesis of the maleimide

derivative, with the aim to purify the final product with column chromatography and a careful selection of the elution solvent (from TLC spotting). By periodically increasing the polarity of the mobile phase we expected to achieve a better separation of the final species.

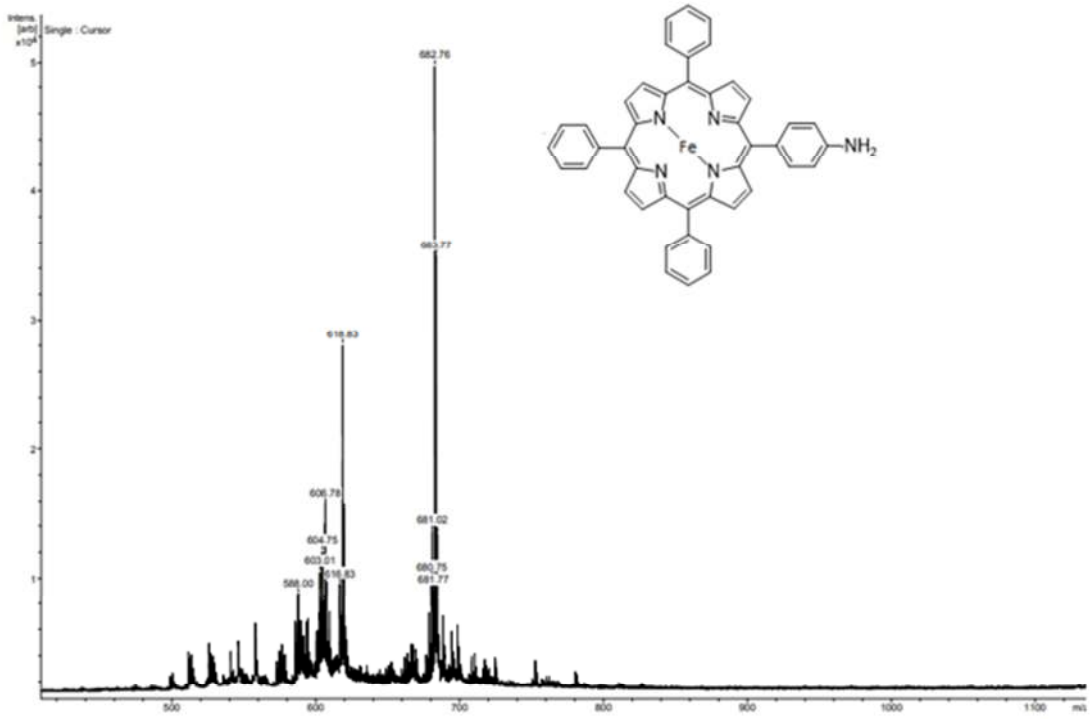

Figure 48 MALDI-TOF spectrum of metallated monoamino-tetraphenylporphyrin.

Fe metalated maleimide porphyrin derivative

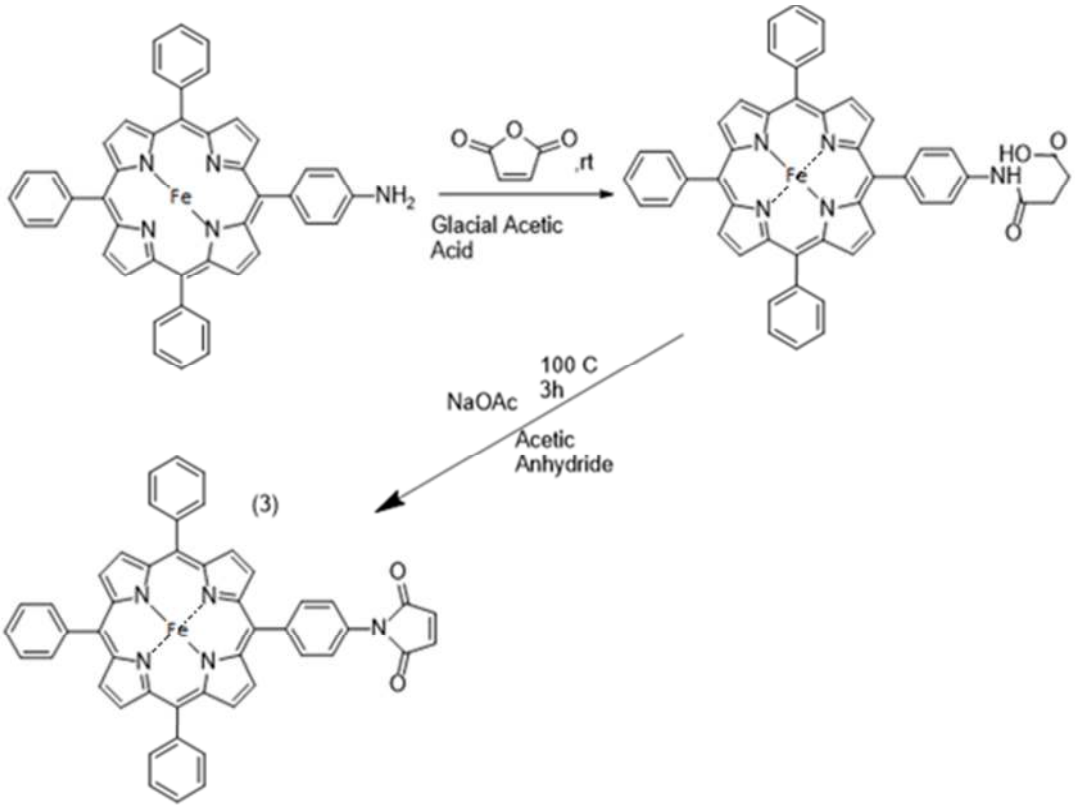

Scheme 1: Synthesis of the Fe-metalated maleimido- tetraphenyl porphyrin

For the synthesis of the the metalated porphyrin maleimide derivative an excess amount of maleic acid was added to the tetraphenyl porphyrin in glacial acetic acid to form the intermediate derivative (2). The excess amount of maleic acid was added to ensure an increased yield of the intermediate (2). The glacial acedic acid was used to form anhydrous conditions during the synthesis. Adding NaOAc and acetic anhydride to the intermediate (2) at 100 ^{o}C yields the maleimide porphyrine derrivative (3) after 3 hours through the mechanisms shown in maleimdie chemistry chapter. The temperature aims to provide the necessary kinetic energy which results in product formation.

After performing the reaction to transform the amine group to a maleimide group, the product was purified via column chromatography with varying solvent polarity starting with DCM (99%) and then switching to DCM/MEOH 99.5/0.5 %, slightly increasing polarity hence causing a faster elution. The eluted band was analysed with MALDI-TOFF MS and although product formation was seen, the majority of the product had formed oxo- and peroxo-dimers due to oxygen presence. Breaking these complexes required treatment with 3N HCl where a chlorine ion binds to the Fe ion as an axial ligand as seen in Figures 49 and 50.

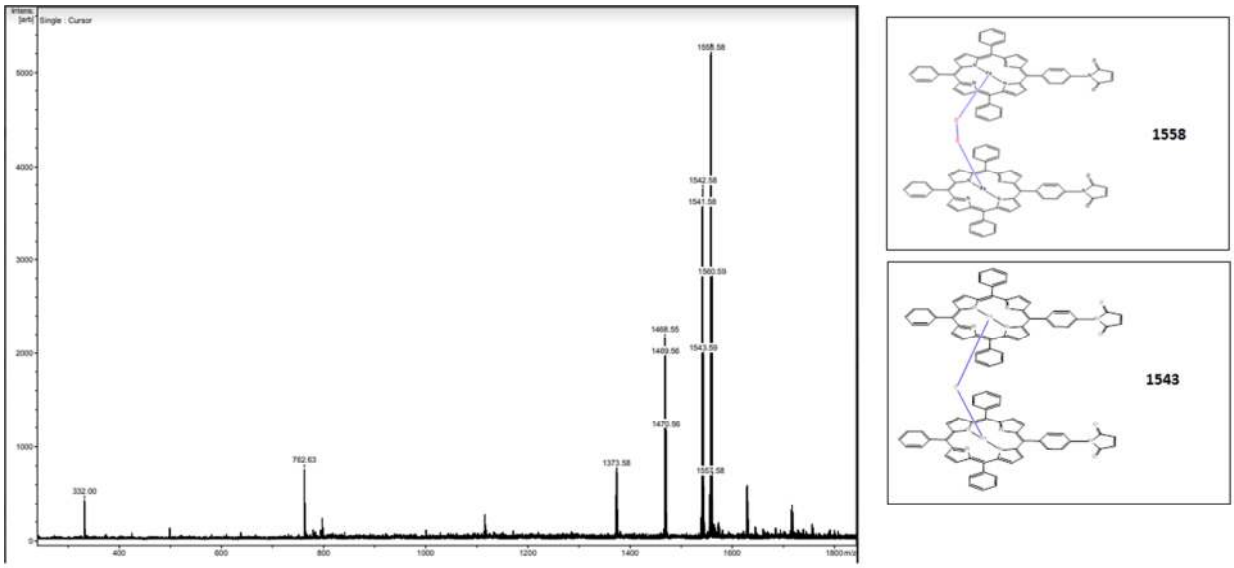

Figure 49 MALDI-TOF of porphyrin-maleimide derrivative.

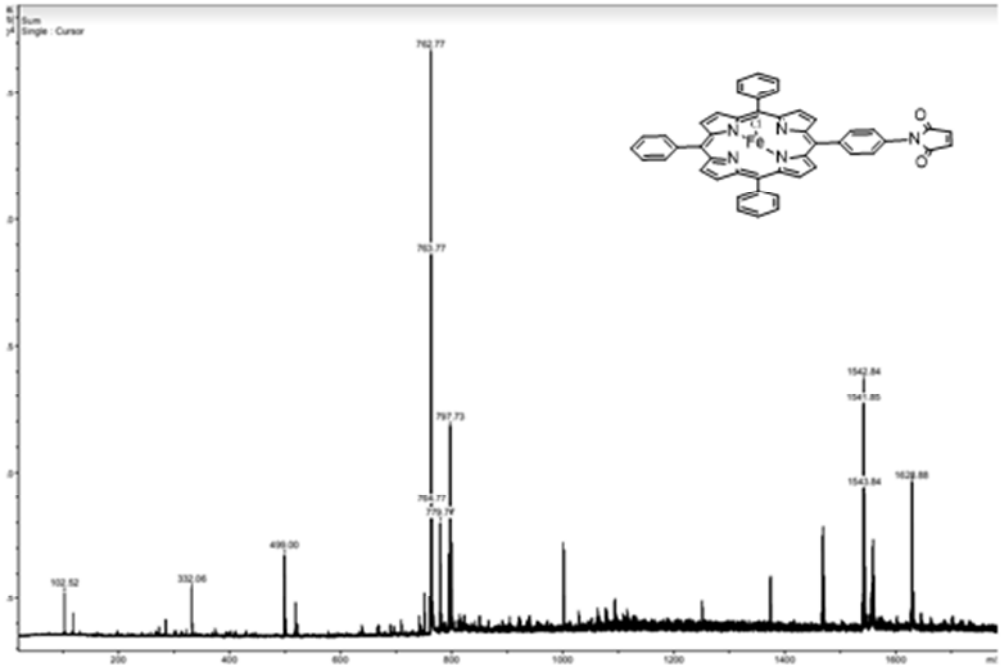

Figure 50 MALDI-TOF of porphyrin-maleimide derrivative after treatment with 3N HCl.

3.0 Materials and methods

Materials

All chemicals were purchased from Aldrich or ACROS and used as received, unless otherwise specified. SDS PAGE chemicals were purchases from Bio-Rad Laboratories.

Analytical Techniques

Gel Permeation Chromatography (GPC)

GPC was used for the characterization of BSA-Porphyrin products, using a mobile phase of 5mM phosphate buffer (pH=7.4), including 10% MeCN. This analytical technique was conducted using Shimadzu VP HPLC system, comprising a DGU-14A solvent degasser, a LC-10AD pump, a CTO-10A column oven, a SIL-10AD auto-injector, a RID-10A refractive index detector and a SPD-10A Shimadzu UV Vis. Spectrometer. All samples were compared to a 0.017 mM BSA in 20mM phosphate buffer solution standard.

MALDI-TOF MS

MALDI-TOFF MS was used for the characterization of BSA-Porphyrin products as well as the porphyrin–maleimide products. This technique was performed on Burker ultrafleXtreme Spectrometer. The matrix applied to BSA-Porphyrin products was a-cyano and the matrix applied to porphyrin maleimide products was trans-2-[3-(4-tert-Butylphenyl)-2-methyl-2-propenylidene] malononitrile.

ESI-MS

ESI-MS was used in an attempt to characterise the BSA-Porphyrin product. This technique was performed on the LCQ Advantage, Thermo Finnigan spectrometer. The sample applied to the spectrometer was treated with alcohol in order to denature the protein moiety and acetic acid in order to apply the necessary charges to the protein for characterisation.

Polyacrylamide Gel Electrophoresis

For electrophoresis a Mini-PROTEAN Tetra Cell was used with a 4% stacking polyacrylamide gel and 10% resolving polyacrylamide gel, under both standard nondenaturing conditions and Laemli denaturing conditions.

Column chromatography

Column chromatography was used for the purification of the porphyrin-maleimide products using a static phase of SiO_2 and a mobile phase varying upon the polarity of the different contaminants

TLC

Thin layer chromatography was used for the identification of a separating solvent by polarity differentiation which would then be used in column chromatography

IR spectroscopy

IR spectroscopy was performed on a Nicolet 6700 ATR FT-IR spectrometer using Omnic software from Thermo Electron Corporation

Methods

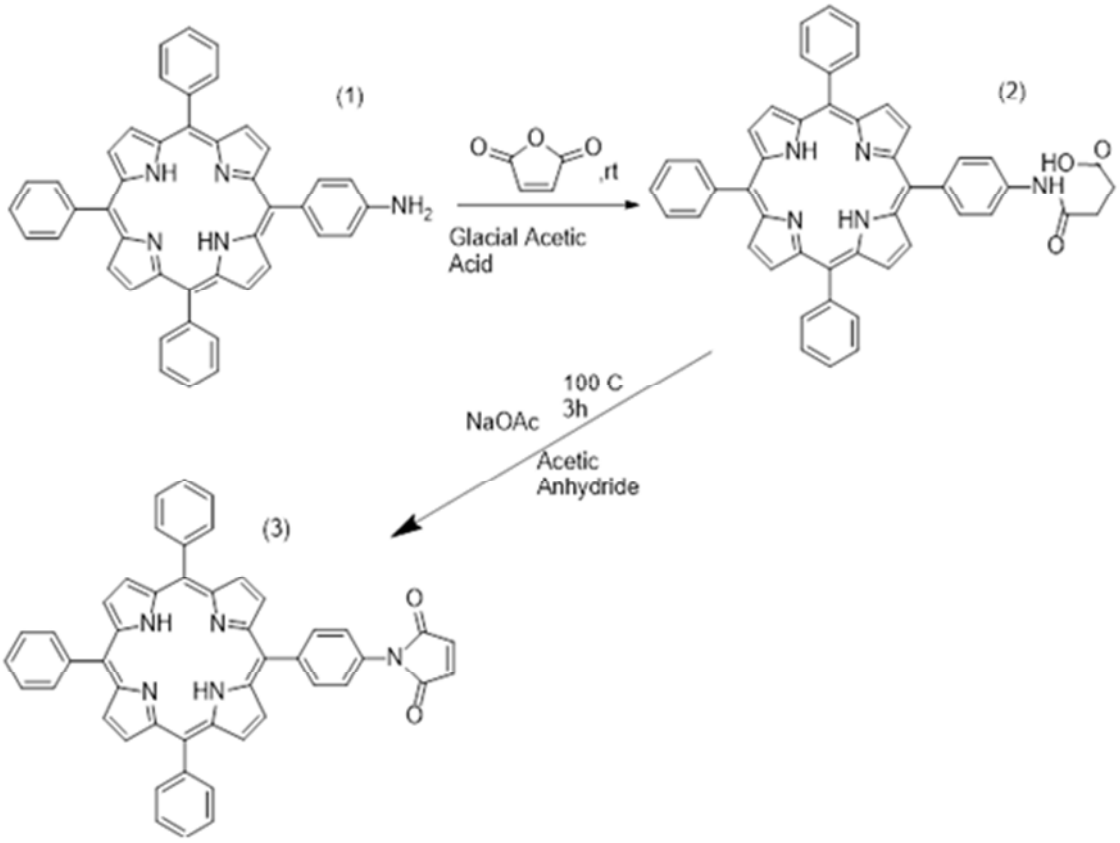

Synthesis of maleimide-porphyrin derivative (3). 100 ml of glacial acetic acid was added to a 500 ml round bottom flask containing 200 mg (0.3 mmol) of monoamino tetraphenyl porphyrin (1) along with 1.5 g (15 mmol) of maleic anhydrite. The reaction was left to stir at room temperature for 12 hours. The solution was distilled and transferred to a 250 ml round bottom flask where 800 mg (9.75 mmol) of sodium acetate was then added along with 50 ml of acetic anhydrite. The solution was left to stir for 2 hours at 100 ^{o}C after which it was

distilled and the final product was purified using column chromatography with silica as the static phase and DCM/hexane 9/1 as the mobile phase. (This synthesis was performed once).[42]

Synthesis of BSA-porphyrin chimera. 2mg (1 eq, 0.03 µmol) of BSA was dissolved in 2.0 ml of phosphate buffer 20 mm at pH 7.2. A solution of 1.9 mg of the porphyrin-maleimide derivative (90 eq, 27 µmol) in 0.200 mL of DMSO was added dropwise to the protein solution and then shaken for 48 hours at room temperature. The solution was first dialyzed (MWCO 10,000) against 20 mm phosphate buffer pH 7.2, 10% DMSO for the depletion of excess porphyrin and subsequently against 20mM phosphate buffer pH 7.2 for the depletion of DMSO. (This synthesis was performed several times)

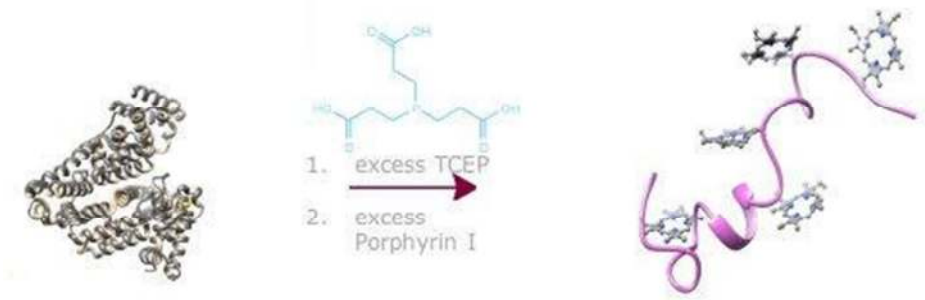

Synthesis Poly-conjugated biohybrid. 2mg (1eq, 0.03 µmol) of BSA was dissolved in 2.0 ml of 20 mM phosphate buffer pH 7.2. 70 eq of TCEP were added (2 eq per disulphide bond) to the solution and left to stir for 1 hour. A solution of the porphyrin-maleimide derivative 1.9 mg (90 eq, 27 µmol) in 0.200 mL of DMSO was added dropwise to the protein solution and then stirred for 48 hours at room temperature. The reaction mixture was first dialyzed (MWCO 10,000) against 20mm phosphate buffer, pH 7.2, 10% DMSO for the depletion of excess porphyrin and subsequently against 20mM phosphate buffer for the depletion of DMSO. (This synthesis was performed 3 times)

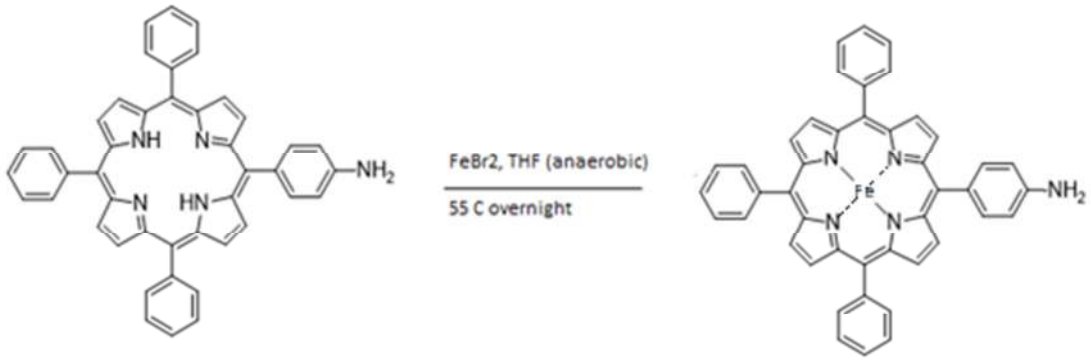

Synthesis of Fe-metalated monoamino-porphyrin derivative. 2.9 equivalents (0.174 mmol) of $FeBr_2$ were added to a shclenk flask under anaerobic conditions using a glove box. The schlenk was then connected to an Argon supply line where it was momentarily uncapped in order to add 1 equivalent (40 mg, 0.06 mmol) of the monoamino porphyrin derivative and 5 ml dry THF. The schlenk flask was capped, and connected to a vacuum pump line. Once a vacuum had been applied, the system was closed by turning the spigot thus keeping a vacuum inside the schlenk. The reaction was left to stir overnight at 55 ^{o}C. TLC spotting and UV-Vis spectroscopy confirmed product formation. Upon uncapping the sclenk the product was introduced to the oxygen containing atmosphere where iron was oxidized from Fe^{II} to Fe^{III} forming oxo- and peroxo- complexes. The solution was distilled and then redissolved in 20 ml of DCM. Liquid-liquid extraction treatment with HCl (25 ml x 4) was necessary to dissociate these complexes adding a chlorine ion as axial ligand. Treatment with water was necessary for the removal of the remaining acid left. The product was purified using column chromatography using silica as the static phase and DCM: MeOH 99.7: 0.3. The separation of the metalated and non-metalated product was not fully achieved after 2 columns according to MALDI-TOFF MS, so the synthesis of the maleimide derivative continued with a slightly contaminated monoamino reactant. (This synthesis was performed once) [43]

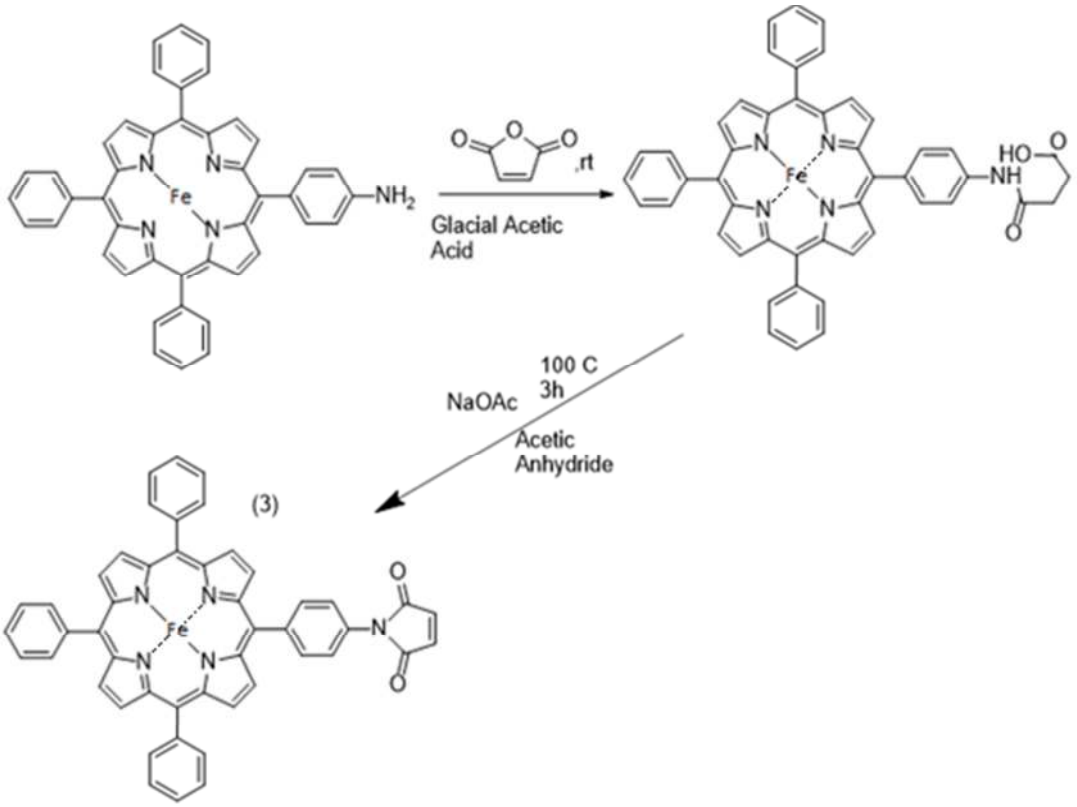

Synthesis of Fe-metalated maleimide-porphyrin derivative (3). 40 mg of the monoamino tetraphenyl porphyrin (1) along with 0.211 g of maleic anhydrite were added to a 250 ml round bottom glass flask containing 14 ml of glacial acetic acid. The reaction was left to stir at room temperature for 12 hours. Afterward the solution was distilled and 800 mg of sodium acetate was added along with 50 ml of acetic anhydrite. The solution was left to stir for 2 hours at 100 ^{o}C after which it was distilled and the final product was purified using column chromatography with silica as the static phase and DCM/methanol 95.5/0.5 as the mobile phase. After the collection of desired band Liquid-liquid extraction treatment with HCl (25mlx4) was performed to break the oxo- and peroxy- complexes, adding a chlorine ion as axial ligand. Treatment with water was necessary for the removal of acid left in solution (This synthesis was performed once).

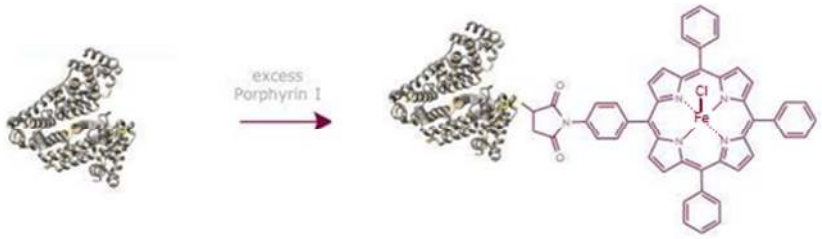

Synthesis of Hybrid hemeprotein, 2 mg (1 eq, 0.03 µmol) of BSA was dissolved in 2.0 ml of 20 mM phosphate buffer, pH 7.2. A solution of 2.1 mg of the Fe-metalated porphyrin-maleimide derivative (90 eq, 26 µmol) in 0.200 mL of DMSO was added dropwise to the protein solution and then gently shaken for 48 hours at room temperature. The reaction mixture was first dialyzed (MWCO 10,000) against 20mM phosphate buffer, pH 7.2, 10% DMSO for the removal of excess porphyrin and subsequently against 20mM phosphate buffer for the removal of DMSO. (Synthesis yet to be executed)

Gel Permeation Chromatography (GPC)

BSA : 25mg of BSA were dissolved in 1ml of phosphate buffer 20mM at PH 7.4. 50µl of that solution is diluted in 950 µl of DD water. The sample was run with a flow rate of 0.05ml/min. This sample was used as a standard to compare with other samples.

Mono-conjugated and Poly-conjugated: 50 µl of phosphate buffer dialyzed sample were diluted with 950µl of DD water. The sample was run with a flow rate of 0.05ml/min.

MALDI-TOF MS :

BSA : 25mg of BSA were dissolved in 1ml 20mM phosphate buffer, pH 7.4. 50µl of the solution were diluted in 950 µl of DD water. The solution was dialyzed 2 times against DD waterv(MWCO 10,000) for 2 hours. The solution was then spotted on the MALDI target plate and left to dry. Once the spot was dry, α-cyano matrix was added to the spot and left to recrystallise with the sample.

Mono-conjugated and poly-conjugated: 50 µl of phosphate buffer dialyzed sample were diluted with 450µl of DD water. The solution was dialyzed two times against DD water (MWCO 10,000) for 2 hours. The solution was then spotted on the MALDI target plate and left to dry. Once the spot was dry, α-cyano matrix was added to the spot and left to recrystallise with the sample.

SDS PAGE electrophoresis: 8µl of undialyzed sample was added to 16 µl of sample buffer and the solution was loaded on a gel comprised of a 4% stacking and a 10% resolving polyacrylamide gel. Voltage of 150 volts was applied to run the electrophoresis

Infrared spectroscopy

Mono-conjugated: 100µl of phosphate dialyzed sample was dialyzed two times against DD water (MWCO 10,000) for 2 hours. The sample was freeze dried. The solid was analysed using BSA as a standard with a 32 cycle analysis.

4.0 Conclusion

The primary purpose of the thesis was the synthesis of hybrid protein-porphyrin chimeras which later on evolved into the synthesis of a hybrid hemeprotein. Our findings confirm the synthesis of the above molecules. Overall we demonstrated that maleimide chemistry could be used without the need of a spacer group between the protein moiety and porphyrin, to facilitate a Michael addition between Cys 34 thiol of BSA and the porphyrin-maleimide. Our work represents the first step toward functional porphyrin-bioconjugates.

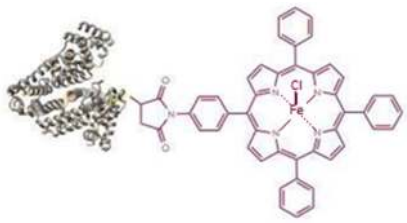

Figure 51 Hybrid hemeprotein

Future research is proposed to include the synthesis and the study of the hybrid hemeprotein functionality. For this to be done, the chlorine ion will have to be removed. This can be achieved by using a reducing agent such as $Na_2S_2O_4$ which will reduce Fe^{+3} to Fe^{+2} thus removing the chlorine ion. This procedure will have to be done in anaerobic environment to avoid reoxidation of the Fe^{+2}. The possibility of it functioning as a catalyst will be determined by a series of experiments. First of all, electron transfer will need to be examined. This can be done by adding the hemeprotein to a solution of electron acceptor such as methyl viologen which changes colour upon redox reactions. If the above experiment gives positive results, the hemoprotein will be tested as a stereoselective catalyst. Furthermore, oxygen carrying properties need to be examined by adding it to an oxygen saturated atmosphere in order for oxygen to bind as an axial ligand. A decrease in O_2 concentration which can be seen using an electrode will signify O_2 binding to the hemoprotein. Upon oxygen addition, oxy- and peroxy- complexes may form if neighbouring amino acids to not provide the right shielding for instance as the distal heme in the globin structure does (left Figure 51)

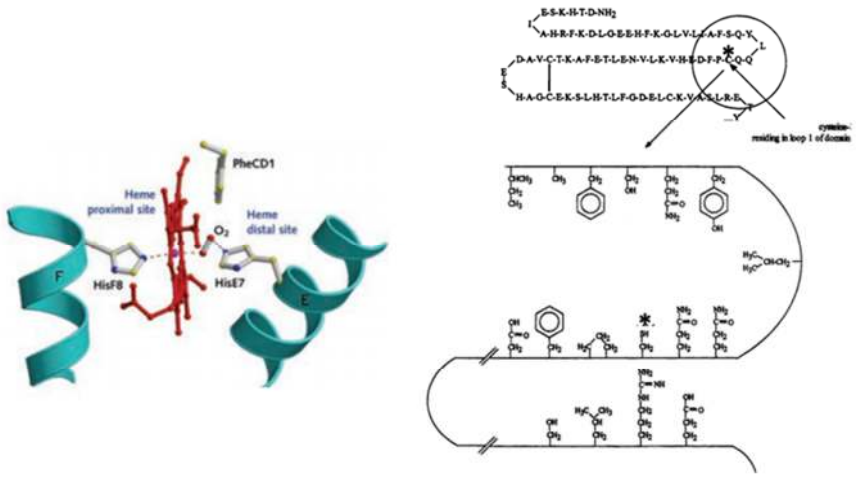

Figure 52 (left) globin structure [3] and (right) neighbouring cys 34 amino acids in BSA [38]

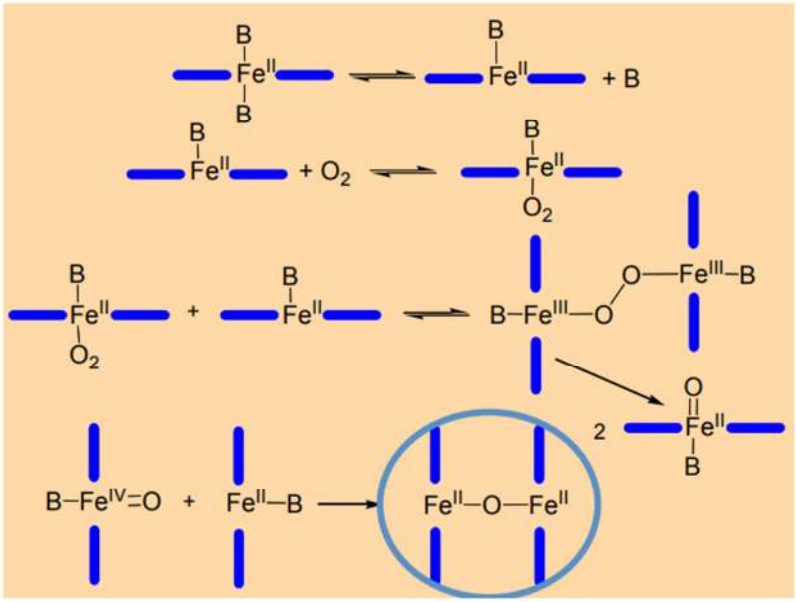

Figure 53 oxy and peroxy complex formation [39]

If no oxy- and peroxy- formation shielding is provided naturally by the surrounding aminoacids (Figure 52 Right), then it will have to be provided synthetically. Synthetic shielding from oxy- and peroxy- complexes can be achieved with many different structural changes to the porphyrin (Figure 55) one of which is the picket fence (Figure 54).

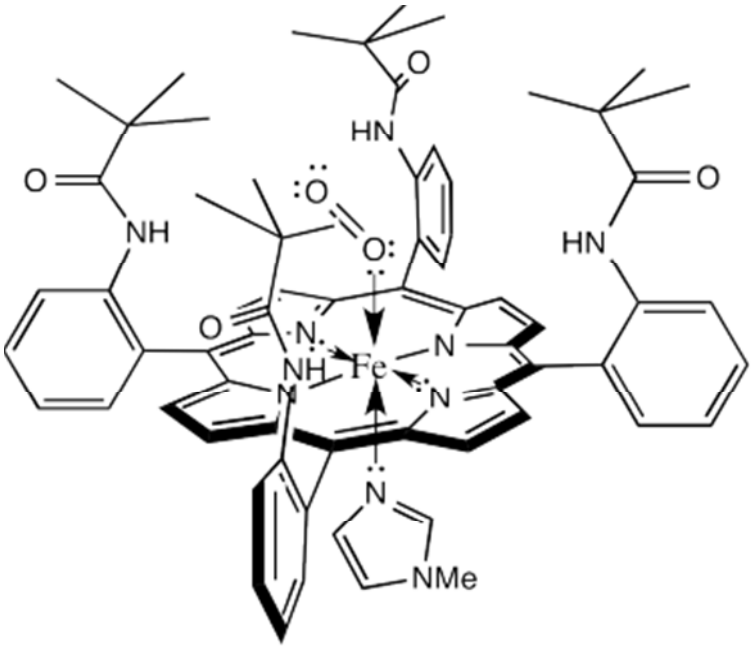

Figure 54 picketfence shielding model

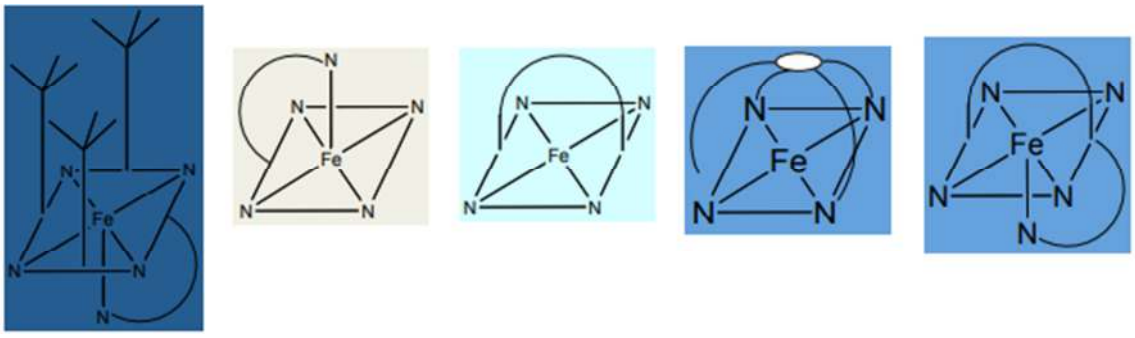

Figure 55 other possible shielding models [34]

The basis for a continuation of this project has been laid out with some solid experimental data. Any future development will need to include the above ideas or even new ideas with different approaches for the synthesis of a functional hybrid hemeprotein that will mimic its bio homologues.

REFERENCES

[1] Wyman J.Jr, Advances in Protein Chemistry , 1948, 4:407-531

[2] Nagarajan D, Sukumaran S, Deka G, Krishuamurthy K, Satreya H, Chandra N , Design of a heme-binding peptide motif adopting a β-hairpin conformation, *Journal Of Biological Chemistry*, 2018, *293*:9412-9422

[3] Pesce A , Bolognesi M, Bocedi A, Ascenzi P, Dewilde S, Moens L, Hankeln T, Burmester T, Neuroglobin and cytoglobin. Fresh blood for the vertebrate globin family, *EMBO Reports*, 2002, *3*:1146-151.

[4] http://www.chemistry.uoc.gr/courses/xhm420, lecture BIC8.

[5] https://www.wiley.com/college/boyer/0470003790/structure/HbMb/EvalText.html.

[6] https://themedicalbiochemistrypage.org/hemoglobin-myoglobin.php.

[7] https://www.rcsb.org/.

[8] https://en.wikipedia.org/wiki/Legume.

[9] Singh S, Varma A, Structure, Function, and Estimation of Leghemoglobin, *Rhizobium Biology and Biotechnology*, 2017, *50*:309-330.

[10] http://www.sbcs.qmul.ac.uk/iubmb/etp/etp4.html.

[11] Alvarez-Paggi D, Hannibal L, Castro M.A, Oviedo-Rouco s, Demicheli V, Tortora V,́ Tomasina R, Radi R, Murgida D.H, Multifunctional Cytochrome c: Learning New Tricks from an Old Dog, *Chemical Reviews*, 2017, *117*:13382-13460.

[12] Brunori M , Giuffre A`, Sarti P, Cytochrome c oxidase, ligands and electrons, *Journal of Inorganic Biochemistry*, 2005 *99*:324–336.

[13] Xia D, Esser L, Tang WK, Zhou F, Zhou Y, Yu L, Yu CA, Structural analysis of cytochrome bc1 complexes: implications to the mechanism of function, *Biochim Biophys Acta*, 2013, *1827*:1278-94.

[14] Kurisu G, Zhang H, Smith JL, Cramer WA, Structure of the cytochrome b6f complex of oxygenic photosynthesis: tuning the cavity, *Science*, 2003, *302*:1009-14.

[15] CécileBreyton, The cytochrome b6f complex: structural studies and comparison with the bc1 complex, *Biochimica et Biophysica Acta (BBA) – Bioenergetics*, 2000*, 1459*:467-474.

[16] Ow YP, Green DR, Hao Z, Mak TW, Cytochrome c: functions beyond respiration, *Nat Rev Mol Cell Biol*, 2008, *7*: 532-42.

[17] Borisov VB, Gennis RB, Hemp J, Verkhovsky MI, The cytochrome bd respiratory oxygen reductases, *Biochim Biophys Acta*, 2011, *1807:*1398-413.

[18] Yang K, Current understanding on cytochrome bd quinol oxidase of Escherichia coli. A mutagenesis, kinetics and spectroscopic study, 2009, Doctor of Philosophy in Biochemistry, University of Illinois at Urbana-Champaign.

[19] Safarian S, Rajendran C, Müller H, Preu J, Langer JD, Ovchinnikov S, Hirose T, Kusumoto T, Sakamoto J, Michel H, Structure of a bd oxidase indicates similar mechanisms for membrane-integrated oxygen reductases, *Science*, 2016, *352*:583-6.

[20] Manikandan P, Nagini S, Cytochrome P450 Structure, Function and Clinical Significance: A Review, *Curr Drug Targets*, 2018, *19*:38-54.

[21] http://www.chemistry.uoc.gr/courses/xhm420, lecture BIC6.

[22] https://www.ebi.ac.uk/interpro/potm/2004_9/Page2.htm.

[23] Zamocky M, Koller F, Understanding the structure and function of catalases:clues from molecular evolution and in vitro mutagenesis, *Progress in Biophysics & Molecular Biology*, 1999, *72*:19-66

[24] Pandey P.V, Awasthi M, Singh S, Tiwari S, Dwivedi U.N, A Comprehensive Review on Function and Application of Plant Peroxidases*, Biochemistry & Analytical Biochemistry*, 2017, 6:308.

[25] Wong DW, Structure and action mechanism of ligninolytic enzymes, *Appl Biochem Biotechnol*, 2009, *157*:174-209.

[26] https://febs.onlinelibrary.wiley.com/doi/epdf/10.1111/febs.13224.

[27] https://www.scribd.com/doc/29643163/Preparation-of-Maleimide.

[28] https://www.thermofisher.com/gr/en/home/life-science/protein-biology/protein-biology-learning-center/protein-biology-resource-library/pierce-protein-methods/sulfhydryl-reactive-crosslinker-chemistry.html.

[29] Shen G, Anand M.F.G, Levicky R, X-ray photoelectron spectroscopy and infrared spectroscopy study of maleimide-activated supports for immobilization of oligodeoxyribonucleotides*, Nucleic Acids Research*, 2004 ,*32*:5973–5980.

[30]https://chem.libretexts.org/Textbook_Maps/Organic_Chemistry/Supplemental_Modules_(Organic_Chemistry)/Reactions/Introduction_to_Bioconjugation.

[31] http://www1.lasalle.edu/~prushan/Abs%20and%20Fluor%20of%20TPPH2.pdf.

[32] Benjamin Le Droumaguet , Kelly Velonia, In Situ ATRP-Mediated Hierarchical Formation of Giant Amphiphile Bionanoreactors, *Angewandte Chemie*, 2008, 47:6263-66.

[33] Aguiar E.C, Silva J.B.P, Ramos M.N, A theoretical study of the vibrational spectrum of maleimide, *Journal of Molecular Structure*, 2011, 993:431-4.

[34] Wagner C.C , Baran E.J , Vibrational Spectra of Bis(L-Methioninato)Copper(II), *Acta Farm. Bonaerense*, 2002, *21*:287-90.

[35] https://www.uniprot.org/uniprot/A0A140T897.

[36] Jones M.W, Mantovani G, Ryan S.M, Wang X, Brayden D.J, Haddleton D.M*, Phosphine-mediated one-pot thiol–ene "click" approach to polymer–protein conjugates, Chemical Communications, 2009, 0:5272-5274.

[37] https://tools.thermofisher.com/content/sfs/manuals/MAN0011216_Ellmans_Reag_UG.pdf

[38] Wang R, Sun S, Bekos E.J, Bright F.V, Dynamics Surrounding Cys-34 in Native, Chemically Denatured, and Silica-Adsorbed Bovine Serum Albumin, *Analytical Chemistry*, 1995, *67*:149-159.

[39] http://www.chemistry.uoc.gr/courses/xhm420, lecture BIC9.

[40] Reedy CJ, Elvekrog MM, Gibney BR, Development of a heme protein structure-electrochemical function database, *Nucleic Acids Research* , 2008, *36*:D307-13.

[41] Karikis K.T, 2014, Synthesis of new porphyrinc omplexes with peripheral sulfur bonds for bioapplication, University of Crete, Heraklion, Greece.

[42] Ruzie C΄,Even P, Ricard D, Roisnel T,Boitrel B, O2 and CO Binding to Tetraaza-Tripodal-Capped Iron(II) Porphyrins, *Inorganic Chemistry* , 2006, *45*:1338−1348.